cmgh
CELLULAR AND MOLECULAR GASTROENTEROLOGY AND HEPATOLOGY

ORIGINAL RESEARCH

Helicobacter pylori–Induced Rev-erbα Fosters Gastric Bacteria Colonization by Impairing Host Innate and Adaptive Defense

Fang-Yuan Mao,[1] Yi-Pin Lv,[1] Chuan-Jie Hao,[1] Yong-Sheng Teng,[1] Yu-Gang Liu,[1] Ping Cheng,[1] Shi-Ming Yang,[2] Weisan Chen,[3] Tao Liu,[4] Quan-Ming Zou,[1] Rui Xie,[5] Jing-Yu Xu,[5] and Yuan Zhuang[1,6]

[1]National Engineering Research Center of Immunological Products, Department of Microbiology and Biochemical Pharmacy, College of Pharmacy and Laboratory Medicine, Third Military Medical University, Chongqing, China; [2]Department of Gastroenterology, XinQiao Hospital, Third Military Medical University, Chongqing, China; [3]La Trobe Institute of Molecular Science, La Trobe University, Bundoora, Australia; [4]Department of Pharmacology, College of Pharmacy and Laboratory Medicine, Third Military Medical University, Chongqing, China; [5]Department of Gastroenterology, Affiliated Hospital of Zunyi Medical University, Zunyi, China; and [6]Department of Gastroenterology, the Affiliated Hospital of Southwest Medical University, Luzhou, China

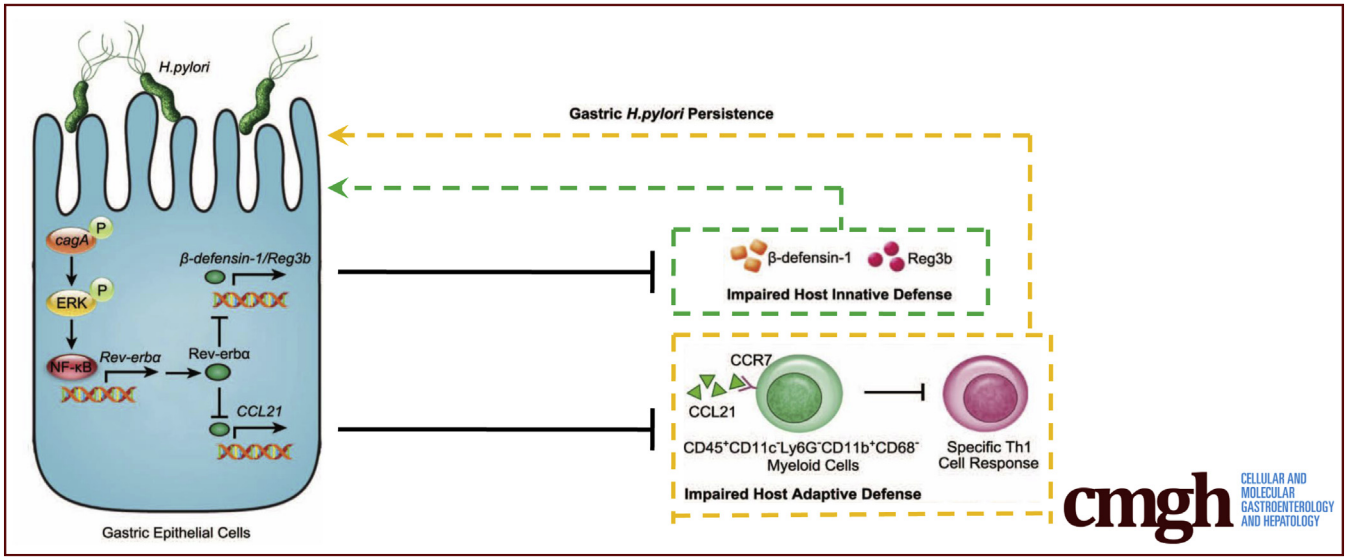

SUMMARY

Helicobacter pylori infection stimulates a novel regulator Rev-erbα that fosters gastric bacterial persistence by suppressing host gene expression required for local innate and adaptive defense against *H pylori*.

BACKGROUND & AIMS: Rev-erbα represents a powerful transcriptional repressor involved in immunity. However, the regulation, function, and clinical relevance of Rev-erbα in *Helicobacter pylori* infection are presently unknown.

METHODS: Rev-erbα was examined in gastric samples from *H pylori*-infected patients and mice. Gastric epithelial cells (GECs) were isolated and infected with *H pylori* for Rev-erbα regulation assays. Gastric tissues from *Rev-erbα*$^{-/-}$ and wild-type (littermate control) mice or these mice adoptively transferred with CD4^{+} T cells from *IFN-γ*$^{-/-}$ and wild-type mice, bone marrow chimera mice and mice with in vivo pharmacological activation or inhibition of Rev-erbα were examined for bacteria colonization. GECs, CD45^{+}CD11c^{-}Ly6G^{-}CD11b^{+}CD68^{-} myeloid cells and CD4^{+} T cells were isolated, stimulated and/or cultured for Rev-erbα function assays.

RESULTS: Rev-erbα was increased in gastric mucosa of *H pylori*-infected patients and mice. *H pylori* induced GECs to express Rev-erbα via the phosphorylated *cagA* that activated ERK signaling pathway to mediate NF-κB directly binding to *Rev-erbα* promoter, which resulted in increased bacteria colonization within gastric mucosa. Mechanistically, Rev-erbα in GECs not only directly suppressed Reg3b and β-defensin-1 expression, which resulted in impaired bactericidal effects against *H pylori* of these antibacterial proteins in vitro and in vivo; but also directly inhibited chemokine CCL21 expression, which led to decreased gastric influx of CD45^{+}CD11c^{-}Ly6G^{-}CD11b^{+}CD68^{-} myeloid cells by CCL21-CCR7-dependent migration and, as a direct consequence, reduced bacterial clearing capacity of *H pylori*-specific Th1 cell response.

CONCLUSIONS: Overall, this study identifies a model involving Rev-erbα, which collectively ensures gastric bacterial persistence by suppressing host gene expression required for local innate and adaptive defense against *H pylori*. *(Cell Mol Gastroenterol Hepatol 2021;12:395–425; https://doi.org/10.1016/j.jcmgh.2021.02.013)*

Keywords: Helicobacter pylori; Rev-erbα; Gastric Epithelial Cells; Host Defense.

Helicobacter pylori is a human pathogen that infects nearly half of the world's population and produces a persistent infection that can lead to gastric ulcers and gastric cancer.[1] Although the persistent colonization of *H pylori* in gastric mucosa remains poorly understood, it is believed that the impaired host defense induced by *H pylori* is a key contributing factor. Gastric epithelial cells (GECs) are not only the first-contacted cell type to exert host defense in gastric mucosa during *H pylori* infection, but also the targets modulated by *H pylori* to re-create gastric microenvironment that may favor gastric *H pylori* persistence. Among the many altered molecules in GECs in response to *H pylori* infection are the nuclear receptors.[2]

Rev-erbα (also called nuclear receptor subfamily 1 group D member 1 [NR1D1]), an orphan nuclear receptor, encoded by *Rev-erbα* and belonged to the thyroid hormone receptor-like superfamily nuclear receptors,[3] is part of the clock-keeping machinery[4] and plays an important role in regulating metabolism[5] and immunity.[6] It can physiologically modulate genes involved in lipid,[7] bile acid,[8] and glucose metabolism[9] in liver and adipose tissues. Under noninfectious conditions, Rev-erbα controls excessive inflammatory responses in liver[4] or pulmonary[10] inflammation. In infectious diseases, Rev-erbα plays roles in antimycobacterial function by repressing interleukin (IL)-10 expression[11,12] and has protective effects in vesicular stomatitis virus–induced encephalitis model through the inhibition of CCL2 expression,[13] respectively. To date, virtually nothing is known about the regulation, function, and clinical relevance of Rev-erbα in GECs during *H pylori* infection in either humans or mice.

In the current study, we have, for the first time, demonstrated a procolonization role of Rev-erbα in *H pylori* infection. Increased Rev-erbα is detected in gastric mucosa of *H pylori*–infected patients and mice, and Rev-erbα expression is induced in GECs by *H pylori* in a *cagA*-dependent manner via extracellular signal-regulated kinase (ERK)–nuclear factor kappa B (NF-κB) pathway activation. On the one hand, Rev-erbα impairs host innate defense to promote gastric *H pylori* infection by directly suppressing the expression of antibacterial proteins Reg3b and β-defensin-1. On the other hand, Rev-erbα directly inhibits CCL21 production, which in turn reduces $CD45^{+}CD11c^{-}Ly6G^{-}CD11b^{+}CD68^{-}$ myeloid cell chemotaxis, as a direct consequence, impairs *H pylori*–specific T helper type 1 (Th1) cell response leading to increasing *H pylori* colonization. Collectively, these data highlight a pathological role for Rev-erbα in persistent *H pylori* infection.

Results

Rev-erbα Is Increased in Gastric Mucosa of H pylori*–Infected Patients and Mice*

Although Rev-erbα was reported to play antimycobacterial role,[11] it is currently not known whether it does also play a role during *H pylori* infection. To evaluate the potential role of Rev-erbα, we first compared the messenger RNA (mRNA) expression profiles of thyroid hormone receptor-like superfamily nuclear receptors in human primary gastric mucosa of *H pylori*–infected and uninfected donors. Among them, Rev-erbα was the most increased one in gastric mucosa infected with *H pylori* compared with paired uninfected counterparts (Figure 1*A*). We then confirmed that, compared with uninfected donors, the overall Rev-erbα mRNA level was higher in gastric mucosa of *H pylori*–infected patients (Figure 1*B*), suggesting an increased Rev-erbα in gastric mucosa of *H pylori*–infected patients.

The presence of *cagA* is strongly associated with the pathogenicity of *H pylori*.[14] Notably, we found that Rev-erbα expression in *cagA*-positive patients was significantly higher than that in *cagA*-negative individuals (Figure 1*C*). Furthermore, a positive correlation between Rev-erbα expression and *H pylori* colonization in gastric mucosa of *H pylori*–infected patients (Figure 1*D*) suggested Rev-erbα induction by *H pylori*. Consistent with our findings in humans, Rev-erbα expression was also much higher in wild-type (WT) *H pylori*–infected but not in *ΔcagA*-infected mice, reaching a peak from 8 weeks postinfection (p.i.) (Figure 1*E*), indicating a key role for *cagA* to induce Rev-erbα during *H pylori* infection in vivo. Furthermore, Western blot analysis (Figure 1*F*), immunohistochemical staining (Figure 1*G*) and immunofluorescence staining (Figure 1*H*) also showed that the level of Rev-erbα protein was higher in gastric mucosa of *cagA*-positive *H pylori*–infected patients and WT *H pylori*–infected mice, compared with either uninfected or *cagA*-negative patients and *ΔcagA*-infected counterparts. Furthermore, infection with WT *H pylori* ex vivo, the levels of Rev-erbα mRNA and protein in human primary gastric mucosa were also significantly increased compared with those in the samples either not infected or infected with *ΔcagA* (Figure 1*I*). Similar observations were made when infecting with *H pylori* 26695 (Figure 1*J*). Taken

Abbreviations used in this paper: **Ab, antibody; BM, bone marrow; ChIP, chromatin immunoprecipitation; CFU, colony-forming units; DMSO, dimethyl sulfoxide; ELISA, enzyme-linked immunosorbent assay; ERK, extracellular signal-regulated kinase; FACS, fluorescence-activated cell sorter; FBS, fetal bovine serum; GEC, gastric epithelial cell; HRP, horseradish peroxidase; IFN-γ, interferon gamma; IL, interleukin; M, monocyte/macrophage; MOI, multiplicity of infection; mRNA, messenger RNA; NC, nonspecific control small interfering RNA; NF-κB, nuclear factor kappa B; p.i., postinfection; PBS, phosphate-buffered saline; PCR, polymerase chain reaction; rDNA, recombinant DNA; siRNA, small interfering RNA; Th1, T helper type 1; WT, wild-type.**

Most current article

2352-345X
https://doi.org/10.1016/j.jcmgh.2021.02.013

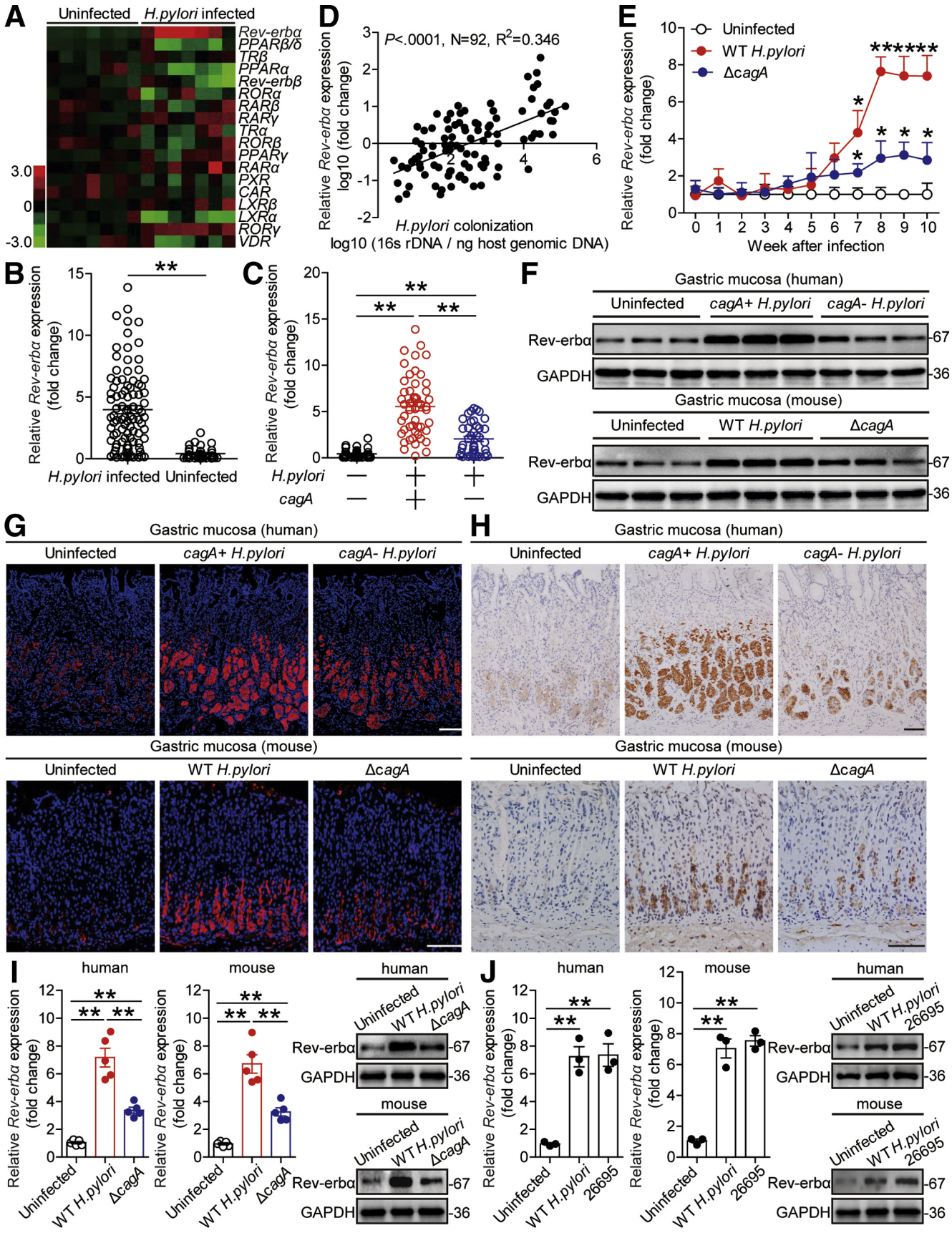
A
Uninfected
H.pylori infected
Rev-erbα
PPARβ/δ
TRβ
PPARα
Rev-erbβ
RORα
RARβ
RARγ
TRα
RORβ
PPARγ
RARα
PXR
CAR
LXRβ
LXRα
RORγ
VDR
3.0
0
-3.0
B
Relative Rev-erbα expression (fold change)
H.pylori infected
Uninfected
C
Relative Rev-erbα expression (fold change)
H.pylori
cagA
D
P<.0001, N=92, R2=0.346
Relative Rev-erbα expression log10 (fold change)
H.pylori colonization log10 (16s rDNA / ng host genomic DNA)
E
Uninfected
WT H.pylori
ΔcagA
Relative Rev-erbα expression (fold change)
Week after infection
F
Gastric mucosa (human)
Uninfected
cagA+ H.pylori
cagA- H.pylori
Rev-erbα
GAPDH
Gastric mucosa (mouse)
Uninfected
WT H.pylori
ΔcagA
G
Gastric mucosa (human)
Uninfected
cagA+ H.pylori
cagA- H.pylori
Gastric mucosa (mouse)
Uninfected
WT H.pylori
ΔcagA
H
Gastric mucosa (human)
Uninfected
cagA+ H.pylori
cagA- H.pylori
Gastric mucosa (mouse)
Uninfected
WT H.pylori
ΔcagA
I
human
mouse
Relative Rev-erbα expression (fold change)
Uninfected
WT H.pylori
ΔcagA
Rev-erbα
GAPDH
J
human
mouse
Relative Rev-erbα expression (fold change)
Uninfected
WT H.pylori
26695
Rev-erbα
GAPDH

together, these findings suggest that Rev-erbα is increased in *H pylori*–infected gastric mucosa of patients and mice.

GECs Infected by H pylori Express Rev-erbα

GECs, the first-contacted cells in gastric mucosa during *H pylori* infection,[14] might be responsible for Rev-erbα expression after *H pylori* infection. Notably, within gastric mucosa of *H pylori*–infected patients, Rev-erbα was expressed in the cytoplasm and nucleus of $CD326^+$ GECs and in the pepsinogen II^+ chief cells in gastric corpus (Figure 2*A*), suggesting that GECs express Rev-erbα in gastric mucosa during *H pylori* infection. We also found that *H pylori* was in contact to the Rev-erbα–expressing cells in gastric mucosa of *H pylori*–infected patients (Figure 2*B*).

Next, to explore the Rev-erbα induction in GECs, we confirmed increased Rev-erbα expression in the nucleus of AGS cells, the cells used to investigate the effects of *H pylori* infection on GECs,[15] infected with *H pylori* (Figure 2*C* and *D*). We further demonstrated that *H pylori*–infected AGS cells (Figure 2*E*) and human primary GECs (Figure 2*F*) increased Rev-erbα expression in a time-dependent and infection dose-dependent manner. Notably, compared with uninfected or *ΔcagA*-infected, WT *H pylori*–infected AGS cells and human primary GECs potently increased Rev-erbα expression (Figure 2*G*). Similar observations were made when other human GEC lines were infected with *H pylori* (Figure 2*H*). Collectively, these results demonstrate that *H pylori* infection induces Rev-erbα expression in GECs.

H pylori Induces GECs to Express Rev-erbα via ERK-NF-κB Pathway

To further explore which signaling pathways might operate in the induction of Rev-erbα in GECs by *H pylori*, we first pretreated AGS cells with corresponding pathway inhibitors and then infected them with *H pylori*. The results showed that only blocking the signal transduction of ERK pathway with inhibitor U0126 effectively decreased Rev-erbα expression (Figure 3*A* and *B*). Furthermore, ERK1/2, a direct ERK pathway downstream substrate, was phosphorylated in the infected AGS cells in an infection dose-dependent and time-dependent manner (Figure 3*C*), which was abolished when pretreated with inhibitor U0126 (Figure 3*D*). Next, to confirm whether *cagA* could induce Rev-erbα via ERK pathway, we infected AGS cells with WT *H pylori* or *ΔcagA*, or transfected AGS cells with *cagA*-pcDNA3.1. We found increased Rev-erbα mRNA and protein and increased ERK1/2 phosphorylation in AGS cells either infected with WT *H pylori* or transfected with *cagA*-pcDNA3.1 compared with those infected with *ΔcagA* or transfected with the vector (pcDNA3.1) (Figure 3*D–F*). Importantly, these were abrogated by pretreatment with the ERK pathway inhibitor U0126 or with *cagA* EPIYA motif phosphorylation inhibitor PP2 (Figure 3*D–F*).[16] To further investigate the effect of *H pylori* on Rev-erbα gene transcription, we synthesized a series of Rev-erbα-luc promoter constructs and cloned them into pGL3-basic vectors. Compared with *ΔcagA* or pcDNA3.1, WT *H pylori* infection or *cagA*-pcDNA3.1 transfection enhanced luciferase activity in AGS cells transfected with full length (–2000/0) Rev-erbα-luc promoter construct plasmid, which was abolished when pretreatment with the ERK pathway inhibitor U0126 (Figure 4*A*). Interestingly, WT *H pylori* infection only enhanced luciferase activity in cells transfected with the Rev-erbα-luc promoter construct flanking regions –2000 to –500 (Figure 4*B*). Further detailed luciferase reporter assay revealed that only the Rev-erbα promoter construct flanking regions –1249 to –1000 produced an increase in cellular luciferase activity upon WT *H pylori* infection (Figure 4*C*). The PROMO tool V.8.3 of TRANSFAC (Beverly, MA) showed that Rev-erbα promoter (–1249/–1000) contains a NF-κB binding site (comprising the sequence: GGGAAATGAC). Subsequently, chromatin immunoprecipitation (ChIP) assay showed that, compared with no infection or *ΔcagA* infection, WT *H pylori* infection significantly increased binding to the Rev-erbα promoter in AGS cells, which was abolished when pretreated with the ERK pathway inhibitor U0126 (Figure 4*D*). Taken together, these findings clearly demonstrate that *cagA*-mediated ERK signaling pathway activation modulates NF-κB's transcriptional regulation on Rev-erbα expression in GECs during *H pylori* infection.

Rev-erbα Suppresses Antibacterial Proteins Reg3b and β-Defensin-1, Leading to Increased Bacterial Burden in Gastric Mucosa During *H pylori* Infection

To evaluate the possible biological effects of Rev-erbα in *H pylori*–associated pathogenesis in vivo, we compared the

Figure 1. (***See previous page***). **Rev-erbα is increased in gastric mucosa of *H pylori*–infected patients and mice.** (*A*) The mRNA expression profiles of thyroid hormone receptor-like superfamily nuclear receptors in human primary gastric mucosa of *H pylori*–infected patients (n = 7) and uninfected donors (n = 7) was analyzed by real-time PCR. (*B*) Rev-erbα mRNA expression in gastric mucosa of *H pylori*–infected (n = 92) and uninfected donors (n = 32) was compared. (*C*) Rev-erbα mRNA expression in gastric mucosa of $cagA^+$ *H pylori*–infected (n = 51), $cagA^-$ *H pylori*–infected (n = 41), and uninfected donors (n = 32) was compared. (*D*) The correlation between Rev-erbα mRNA expression and *H pylori* colonization in gastric mucosa of *H pylori*–infected patients was analyzed with the Pearson r analyze ($R^2 = 0.3460$, *P* value < .0001) (*E*) Dynamic changes of Rev-erbα mRNA expression in gastric mucosa of WT *H pylori*–infected, *ΔcagA*–infected, and uninfected mice. n = 5 per group per time point in *E*. (*F–H*) Rev-erbα protein in gastric corpus of $cagA^+$ *H pylori*–infected, $cagA^-$ *H pylori*–infected, and uninfected donors or in gastric corpus of WT *H pylori*–infected, *ΔcagA*-infected, and uninfected mice 8 weeks p.i. was analyzed by (*F*) Western blot, (*G*) immunohistochemical staining, and (*H*) immunofluorescence staining. Scale bars: 100 μm. (*I*) Rev-erbα mRNA expression and Rev-erbα protein in human or mouse primary gastric mucosa from uninfected donors infected with WT *H pylori* or *ΔcagA* ex vivo analyzed by real-time PCR and Western blot (n = 5). (*J*) Rev-erbα mRNA expression and Rev-erbα protein in human or mouse primary gastric mucosa from uninfected donors infected with WT *H pylori* or *H pylori* 26695 ex vivo analyzed by real-time PCR and Western blot (n = 3). **P* < .05, ***P* < .01 for groups connected by horizontal lines, or compared with uninfected mice.

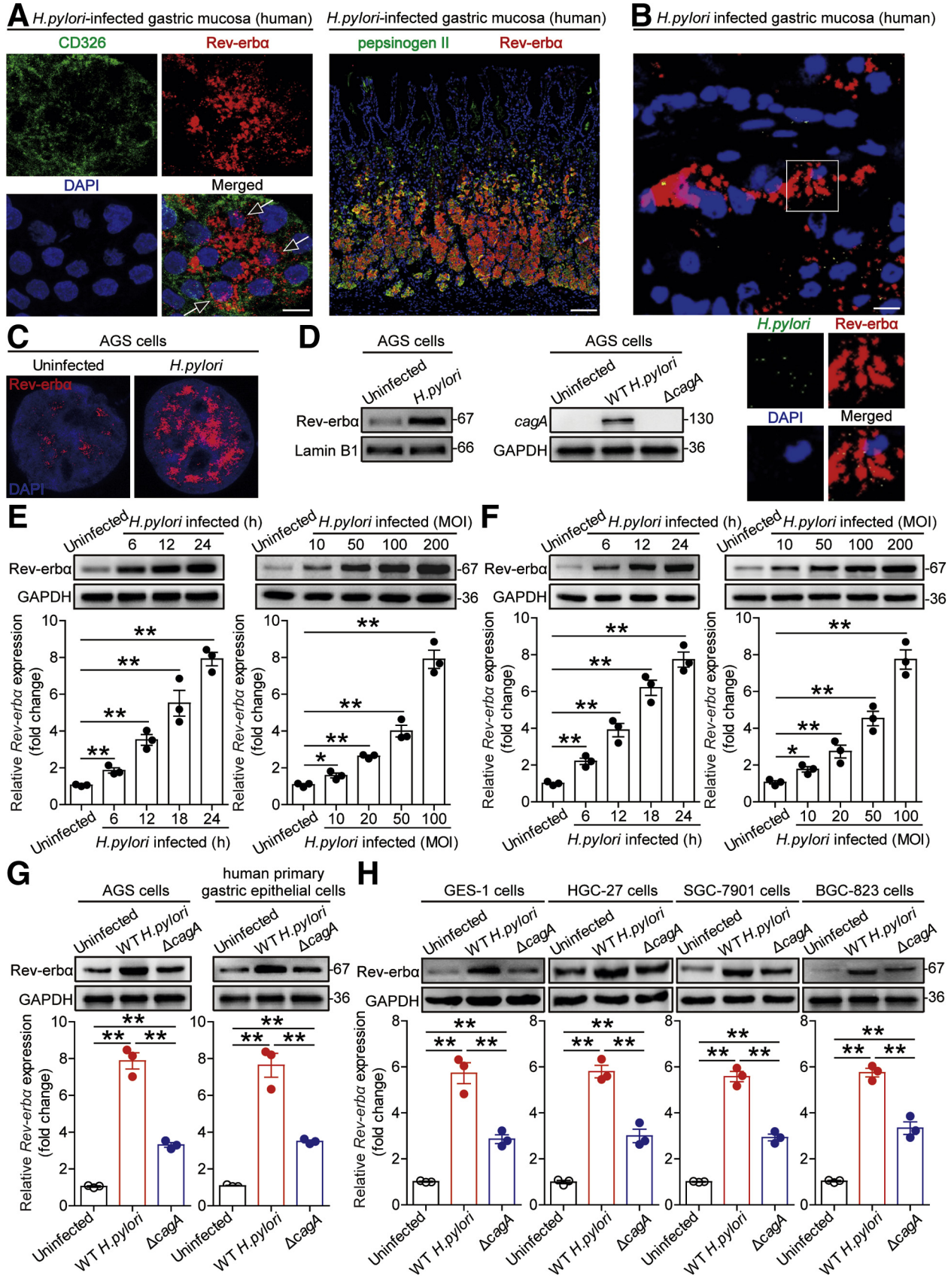
A
H.pylori-infected gastric mucosa (human)
CD326
Rev-erbα
DAPI
Merged
H.pylori-infected gastric mucosa (human)
pepsinogen II
Rev-erbα
B
H.pylori infected gastric mucosa (human)
C
AGS cells
Uninfected
H.pylori
Rev-erbα
DAPI
D
AGS cells
Uninfected
H.pylori
Rev-erbα
Lamin B1
67
66
AGS cells
Uninfected
WT H.pylori
ΔcagA
cagA
GAPDH
130
36
H.pylori
Rev-erbα
DAPI
Merged
E
Uninfected
H.pylori infected (h)
6 12 24
Uninfected
H.pylori infected (MOI)
10 50 100 200
Rev-erbα
GAPDH
67
36
Relative Rev-erbα expression (fold change)
Uninfected 6 12 18 24
H.pylori infected (h)
Uninfected 10 20 50 100
H.pylori infected (MOI)
F
Uninfected
H.pylori infected (h)
6 12 24
Uninfected
H.pylori infected (MOI)
10 50 100 200
Rev-erbα
GAPDH
67
36
Relative Rev-erbα expression (fold change)
Uninfected 6 12 18 24
H.pylori infected (h)
Uninfected 10 20 50 100
H.pylori infected (MOI)
G
AGS cells
human primary gastric epithelial cells
Uninfected
WT H.pylori
ΔcagA
Rev-erbα
GAPDH
67
36
Relative Rev-erbα expression (fold change)
Uninfected
WT H.pylori
ΔcagA
H
GES-1 cells
HGC-27 cells
SGC-7901 cells
BGC-823 cells
Uninfected
WT H.pylori
ΔcagA
Rev-erbα
GAPDH
67
36
Relative Rev-erbα expression (fold change)
Uninfected
WT H.pylori
ΔcagA

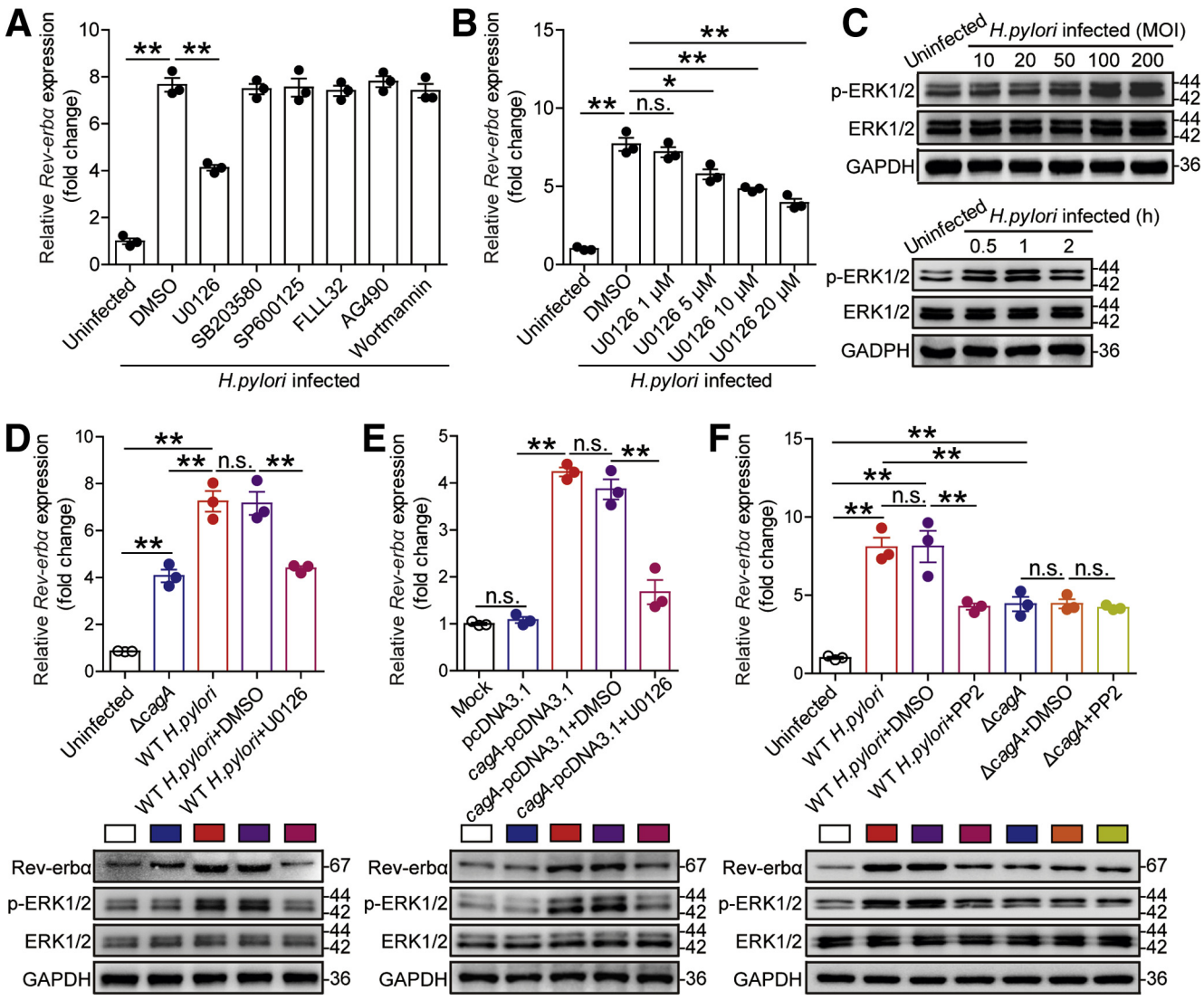

Figure 3. *H pylori* induces Rev-erbα expression via the phosphorylated *cagA*-activated ERK signaling pathway. (*A*, *B*) AGS cells were pretreated with signal pathway inhibitors and then stimulated with WT *H pylori* (MOI = 100) for 24 hours. Rev-erbα mRNA expression in AGS cells was compared (n = 3). (*C*) AGS cells were stimulated with WT *H pylori* with different MOI (6 hours) or at different time point (MOI = 100). ERK1/2 and p-ERK1/2 proteins were analyzed by Western blot. (*D*) AGS cells were pretreated with or without U0126 and then infected with WT *H pylori* or *ΔcagA* (MOI = 100) for 24 hours. Rev-erbα mRNA expression in these cells was compared (n = 3). Rev-erbα, ERK1/2, and p-ERK1/2 proteins were analyzed by Western blot. (*E*) AGS cells were transfected with plasmids pcDNA3.1 or *cagA*-pcDNA3.1 for 24 hours, then treated with or without U0126 for 2 hours and cultured for an additional 24 hours. Rev-erbα mRNA expression in these cells was compared (n = 3). Rev-erbα, ERK1/2, and p-ERK1/2 proteins were analyzed by Western blot. (*F*) AGS cells were pretreated with or without PP2 and then infected with WT *H pylori* or *ΔcagA* (MOI = 100) for 24 hours. Rev-erbα mRNA expression in these cells was compared (n = 3). Rev-erbα, ERK1/2 and p-ERK1/2 proteins were analyzed by Western blot. **P* < .05, ***P* < .01, n.s. *P* > .05 for groups connected by horizontal lines.

Figure 2. (***See previous page***). **GECs express Rev-erbα during *H pylori* infection.** (*A*) Representative immunofluorescence staining images showing Rev-erbα expression (red) in cytoplasm and nucleus (arrow) of $CD326^+$ cells (green) and Rev-erbα–expressing (*red*) pepsinogen II^+ chief cells (green) in gastric corpus of *H pylori*–infected patients. Scale bars: 10 μm or 100 μm. (*B*) Representative immunofluorescence staining images showing Rev-erbα–expressing (red) cells and *H pylori* (green) colonization in gastric mucosa of *H pylori*–infected patients. Scale bars: 10 μm. (*C*) Representative immunofluorescence staining images showing Rev-erbα expression (red) in WT *H pylori*–infected, and uninfected AGS cells (MOI = 100, 6 hours). Scale bars: 1 μm. (*D*) Rev-erbα expression in the nucleus of WT *H pylori*–infected, and uninfected AGS cells (MOI = 100, 24 hours) was analyzed by Western blot. The expression of *cagA* protein in AGS cells infected with WT *H pylori* or *ΔcagA* (MOI = 100, 24 hours) was analyzed by Western blot. (*E*, *F*) Rev-erbα mRNA expression and Rev-erbα protein in WT *H pylori*–infected and (*E*) uninfected AGS cells or (*F*) human primary GECs at different time point (MOI = 100) or with different MOI (24 hours) were analyzed by real-time PCR or Western blot (n = 3). (*G*) Rev-erbα mRNA expression and Rev-erbα protein in WT *H pylori*–infected, *ΔcagA*-infected, and uninfected AGS cells or human primary GECs (MOI = 100, 24 hours) were analyzed by real-time PCR and Western blot (n = 3). (*H*) Rev-erbα expression in WT *H pylori*–infected, *ΔcagA*-infected, and uninfected GES-1 cells, HGC-27 cells, SGC-7901 cells, and BGC-823 cells (MOI = 100, 24 hours) was analyzed by real-time PCR and Western blot (n = 3). **P* < .05, ***P* < .01 for groups connected by horizontal lines.

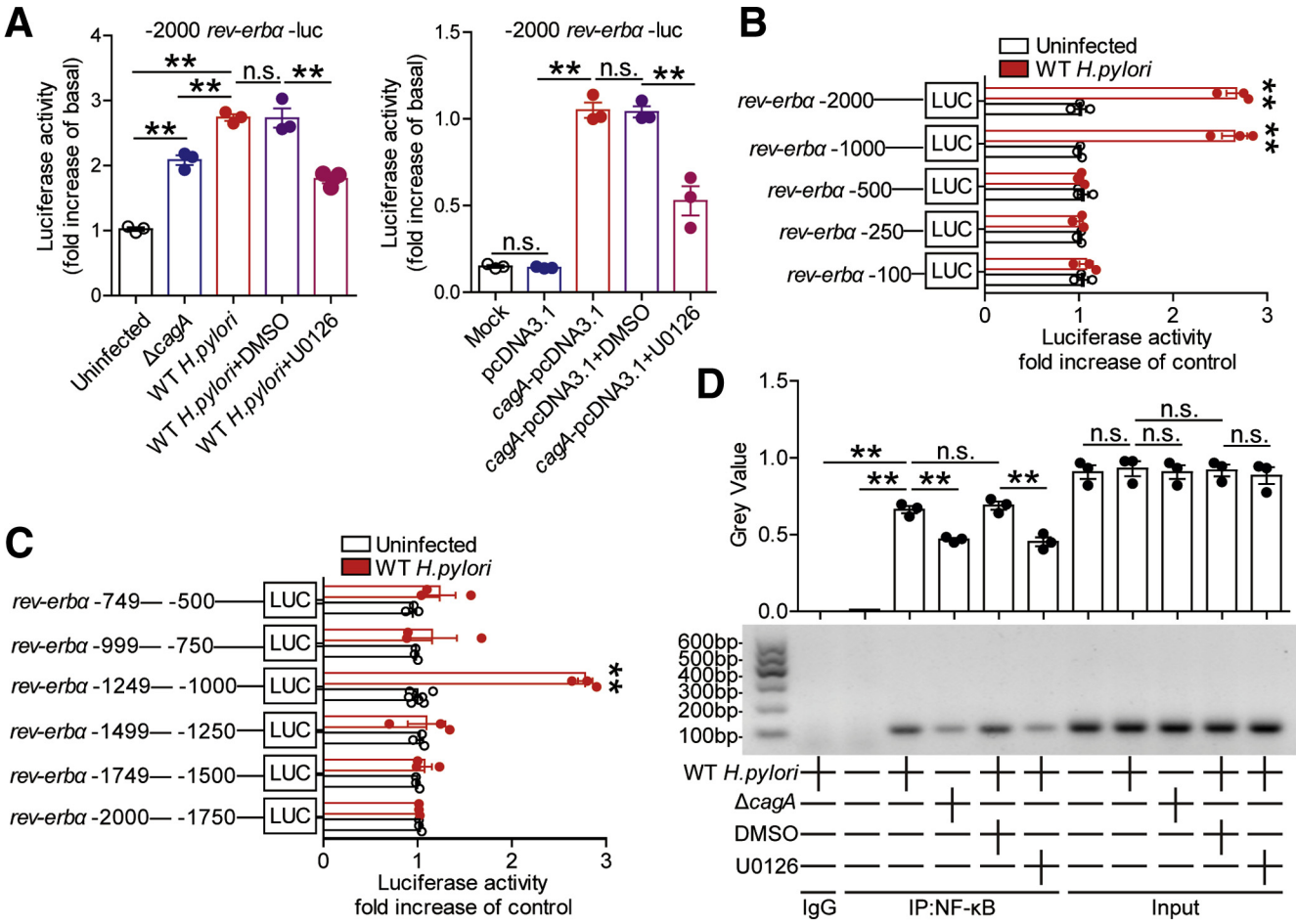

Figure 4. *H pylori* induces Rev-erbα expression via ERK-NF-κB pathway. (*A*) AGS cells were transfected with luciferase reporter constructs containing the *Rev-erbα*-luc promoter for 4 hours. Luciferase activity was measured to assess promoter activity after WT *H pylori* (pretreated with or without U0126) or *ΔcagA* infection (MOI = 100) for 24 hours (n = 3). AGS cells were cotransfected with *Rev-erbα*-luc construct and *cagA*-pcDNA3.1 (pretreated with or without U0126) or pcDNA3.1 (control vector) for 48 hours. Luciferase activity was measured to assess Rev-erbα promoter activity (n = 3). (*B*, *C*) AGS cells were transfected with *Rev-erbα*-luc constructs for 4 hours. Luciferase activity was measured to assess promoter activity after WT *H pylori* infection (MOI = 100) for 24 hours (n = 3). (*D*) Representative data and statistical analysis of ChIP assay in AGS cells infected with WT *H pylori* (pretreated with or without U0126) or Δ*cagA*, followed by regular PCR with primers designed for NF-κB binding site of Rev-erbα promoter region (n = 3). $^{**}P < .01$, n.s. $P > .05$ for groups connected by horizontal lines, or compared with uninfected cells.

levels of bacterial colonization in gastric mucosa 8 weeks p.i. in WT and *Rev-erbα*$^{-/-}$ mice, and found that lacking endogenous Rev-erbα in *Rev-erbα*$^{-/-}$ mice effectively reduced *H pylori* colonization when compared with that in WT mice (Figure 5*A*). Next, we again compared bacterial colonization in mice with in vivo pharmacological activation or inhibition of Rev-erbα by injecting exogenous Rev-erbα agonist or Rev-erbα antagonist and found that activation of Rev-erbα significantly increased *H pylori* colonization; conversely, inhibition of Rev-erbα significantly reduced gastric colonization when compared with that in control mice (Figure 5*B*). Finally, consistent with our previous findings that GECs are the source cells that express Rev-erbα in gastric mucosa during *H pylori* infection (Figure 2), by generating bone marrow (BM) chimera mice, we found that non–BM-derived Rev-erbα–expressing cells (including GECs) largely contribute to increasing bacterial colonization in this model (Figure 5*C*). Taken together, our data demonstrate that Rev-erbα plays an essential role in promoting bacterial colonization in vivo.

Given powerful transcriptional repressing effects of Rev-erbα was observed in other infectious diseases,[11,13] we hypothesized that Rev-erbα might exert inhibiting effects on genes encoding proteins contributing to host defense. The β-defensins[17] and Reg3 proteins[18] play roles in mucosal defense during *H pylori* infection. We therefore screened these proteins in gastric mucosa 8 weeks p.i. in WT and *Rev-erbα*$^{-/-}$ mice, and found that lacking Rev-erbα in *Rev-erbα*$^{-/-}$ mice led to increased Reg3b and β-defensin-1 expression when compared with that in WT mice (Figure 5*D* and *E*). Similar observations were made when using in vivo pharmacological activation or inhibition of Rev-erbα experiments (Figure 5*F*). Again, BM chimera experiments confirmed that non–BM-derived Rev-erbα–expressing cells

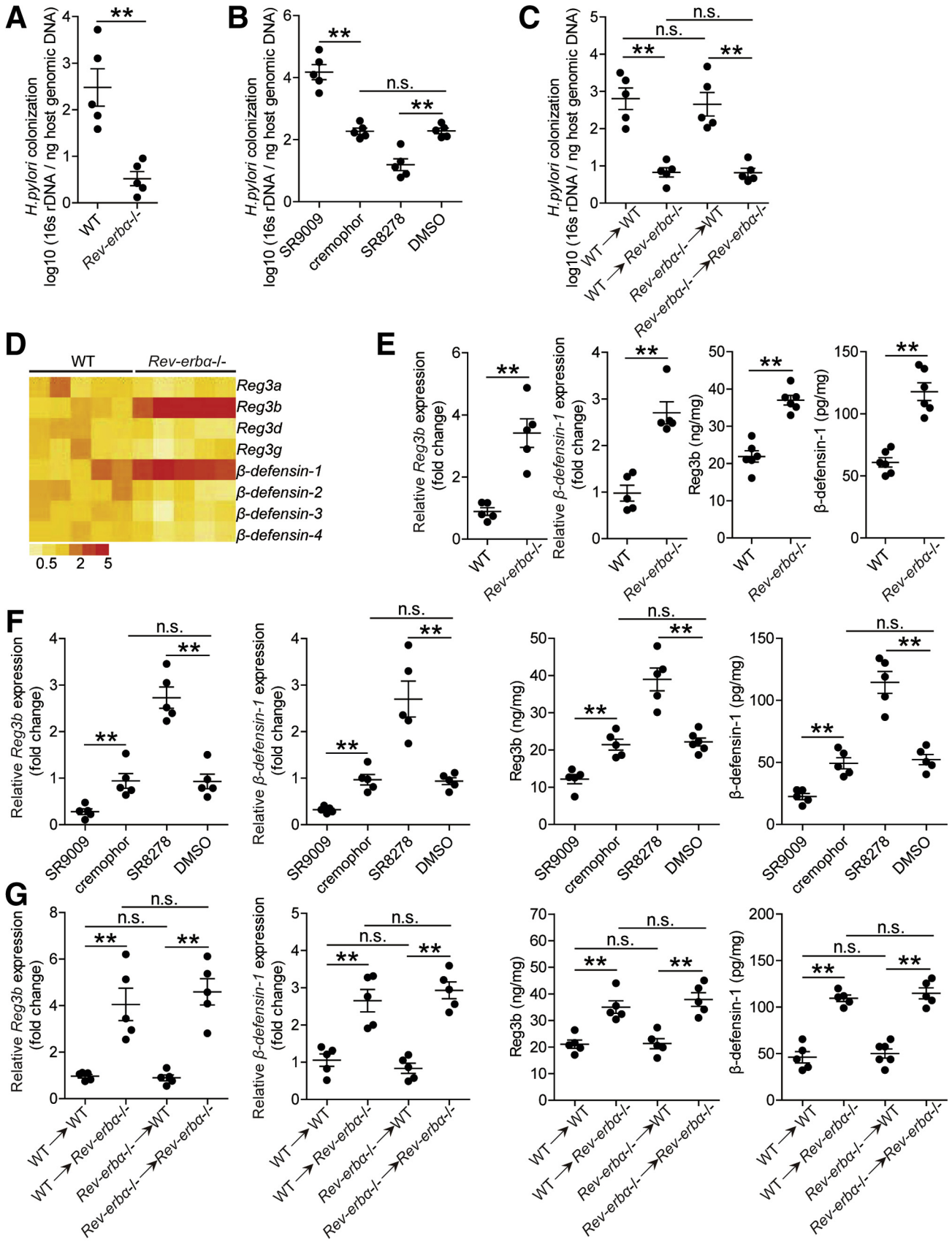
A
H.pylori colonization
log10 (16s rDNA / ng host genomic DNA)
WT
Rev-erbα-/-
B
SR9009
cremophor
SR8278
DMSO
C
WT → WT
Rev-erbα-/- → WT
WT → Rev-erbα-/-
Rev-erbα-/- → Rev-erbα-/-
D
WT
Rev-erbα-/-
Reg3a
Reg3b
Reg3d
Reg3g
β-defensin-1
β-defensin-2
β-defensin-3
β-defensin-4
0.5 2 5
E
Relative Reg3b expression (fold change)
Relative β-defensin-1 expression (fold change)
Reg3b (ng/mg)
β-defensin-1 (pg/mg)
F
G
n.s.
**

were largely responsible for inhibiting Reg3b and β-defensin-1 in gastric mucosa during *H pylori* infection (Figure 5*G*). Furthermore, similar observations were made when analyzing Reg3b and β-defensin-1 protein by immunohistochemical staining (Figure 6*A*–*C*).

To further investigate the roles of Reg3b and β-defensin-1 in *H pylori* infection, we performed in vitro and in vivo bactericidal assay. First, in vitro bactericidal assay showed that Reg3b and β-defensin-1 exerted killing activity against *H pylori* in a time-dependent and infection dose-dependent manner (Figure 6*D*). Next, in vivo gain-of-function experiments showed that Reg3b or β-defensin-1 administration significantly reduced *H pylori* colonization in gastric mucosa of WT mice (Figure 6*E*). As for the negative correlations between Rev-erbα and Reg3b/β-defensin-1 (Figure 6*F*) in gastric mucosa of *H pylori*–infected mice and host defense against *H pylori* from GEC-derived antibacterial proteins,[17] we next found that, upon *H pylori* infection, GECs derived from *Rev-erbα*$^{-/-}$ mice produced more Reg3b and β-defensin-1 compared with those from WT mice (Figure 7*A*), and that supernatants from *H pylori*–infected GECs of *Rev-erbα*$^{-/-}$ mice exerted more pronounced killing activity against *H pylori* than those of WT mice (Figure 7*B*), which could be abrogated by blocking Reg3b or β-defensin-1 (Figure 7*B*). Finally, to explore the molecule mechanism of β-defensin-1 inhibition in GECs by Rev-erbα (human have no *Reg3b* gene), we performed luciferase reporter assays, and the results showed decreased activity of β-defensin-1-luc when transfected together with the *Rev-erbα*-pcDNA3.1, and retrieved activity when the Rev-erbα binding site on the β-defensin-1 promoter was mutated (Figure 7*C*); further ChIP assays showed that WT *H pylori* infection significantly increased binding activity to the β-defensin-1 promoter with the Rev-erbα antibodies (Abs) (Figure 7*D*), together suggesting that in WT *H pylori*–infected AGS cells, Rev-erbα directly inhibited β-defensin-1 expression. Taken together, our data demonstrate that, in *H pylori*–infected gastric mucosa, Rev-erbα in GECs inhibits Reg3b and β-defensin-1 directly, which likely contributes to bacterial persistence.

Rev-erbα Inhibits CD45$^+$CD11c$^-$Ly6G$^-$CD11b$^+$CD68$^-$ Myeloid Cell Accumulation and CCL21 Production in Gastric Mucosa During H pylori *Infection*

To investigate whether increased Rev-erbα regulated immune cell infiltration into the gastric mucosa during *H pylori* infection, we compared the levels of CD45$^+$CD11c$^+$Ly6G$^-$ dendritic cells, CD45$^+$CD11c$^-$Ly6G$^+$ neutrophils, CD45$^+$CD11c$^-$Ly6G$^-$CD3$^+$NK1.1$^-$ T cells, CD45$^+$CD11c$^-$Ly6G$^-$CD3$^-$NK1.1$^+$ natural killer cells, CD45$^+$CD11c$^-$Ly6G$^-$CD3$^-$NK1.1$^-$CD19$^+$ B cells, and CD45$^+$CD11c$^-$Ly6G$^-$CD11b$^+$CD68$^-$ myeloid cells in gastric mucosa 8 weeks p.i. in WT and *Rev-erbα*$^{-/-}$ mice, and found that lacking Rev-erbα in *Rev-erbα*$^{-/-}$ mice only led to increased CD45$^+$CD11c$^-$Ly6G$^-$CD11b$^+$CD68$^-$ myeloid cells (Figure 8*A*–*C*). These results were also confirmed by our in vivo pharmacological activation or inhibition of Rev-erbα experiments and BM chimera experiments in which non–BM-derived Rev-erbα–expressing cells were largely responsible for this myeloid cell reduction in gastric mucosa during *H pylori* infection (Figure 8*D* and *E*). Similar observations were made when analyzing the number of CD45$^+$CD11c$^-$Ly6G$^-$CD11b$^+$CD68$^-$ myeloid cells per million total cells in gastric mucosa (Figure 8*C*–*E*). Notably, compared with WT mice, Ly6C$^+$CD11b$^+$ myeloid cell accumulation was higher in gastric mucosa of *H pylori*–infected *Rev-erbα*$^{-/-}$ mice 8 weeks p.i. (Figure 8*F*). Furthermore, blood, spleen, or BM CD45$^+$CD11c$^-$Ly6G$^-$CD11b$^+$CD68$^-$ myeloid cell levels were not altered in these mouse models above (Figure 9). Taken together, our data demonstrate that Rev-erbα plays an essential role in the inhibition of CD45$^+$CD11c$^-$Ly6G$^-$CD11b$^+$CD68$^-$ myeloid cell accumulation in gastric mucosa during *H pylori* infection.

Chemotaxis plays important roles in immune cell migration. We were therefore interested to know if Rev-erbα regulated chemokine production in gastric mucosa. We screened chemokines in gastric mucosa 8 weeks p.i. in WT and *Rev-erbα*$^{-/-}$ mice, and found that only CCL21 expression was increased in *Rev-erbα*$^{-/-}$ mice (Figure 10*A* and *B*). Again, these results were confirmed by our in vivo pharmacological activation or inhibition of Rev-erbα experiments and BM chimera experiments in which non–BM-derived Rev-erbα–expressing cells were largely responsible for CCL21 inhibition in gastric mucosa during *H pylori* infection (Figure 10*C* and *D*). Taken together, our data demonstrate that Rev-erbα plays an essential role in inhibiting CCL21 production in gastric mucosa during *H pylori* infection.

To understand the negative correlation between Rev-erbα and CCL21 (Figure 10*E*) and CCL21 expression in CD326$^+$ cells (Figure 10*F*) in gastric mucosa of *H pylori*–infected patients and mice, we then explored the molecular mechanism by which Rev-erbα down-modulate CCL21 expression in GECs. Luciferase reporter assay showed decreased activity of CCL21-luc when transfected

Figure 5. (***See previous page***). **Rev-erbα suppresses antibacterial proteins Reg3b and β-defensin-1 and increases bacterial burden in gastric mucosa during *H pylori* infection.** (*A*–*C*) The bacteria colonization in (*A*) gastric mucosa of WT *H pylori*–infected WT and *Rev-erbα*$^{-/-}$ mice, (*B*) gastric mucosa of WT *H pylori*–infected mice with in vivo by injecting Rev-erbα agonist SR9009 or cremophor control, or Rev-erbα antagonist SR8278 or DMSO control, or (*C*) gastric mucosa of WT *H pylori*–infected BM chimera mice was compared 8 weeks p.i. (n = 5). (*D*) The mRNA expression profiles of β-defensins and Reg3 proteins in gastric mucosa of WT *H pylori*–infected WT and *Rev-erbα*$^{-/-}$ mice 8 weeks p.i. was analyzed by real-time PCR (n = 5). (*E*–*G*) The mRNA expression or the concentrations of Reg3b and β-defensin-1 in (*E*) gastric mucosa of WT *H pylori*–infected WT and *Rev-erbα*$^{-/-}$ mice, (*F*) gastric mucosa of WT *H pylori*–infected mice with in vivo by injecting Rev-erbα agonist SR9009 or cremophor control, or Rev-erbα antagonist SR8278 or DMSO control, or (*G*) gastric mucosa of WT *H pylori*–infected BM chimera mice was compared 8 weeks p.i. (n = 5). $^{**}P < .01$, n.s. $P > .05$ for groups connected by horizontal lines.

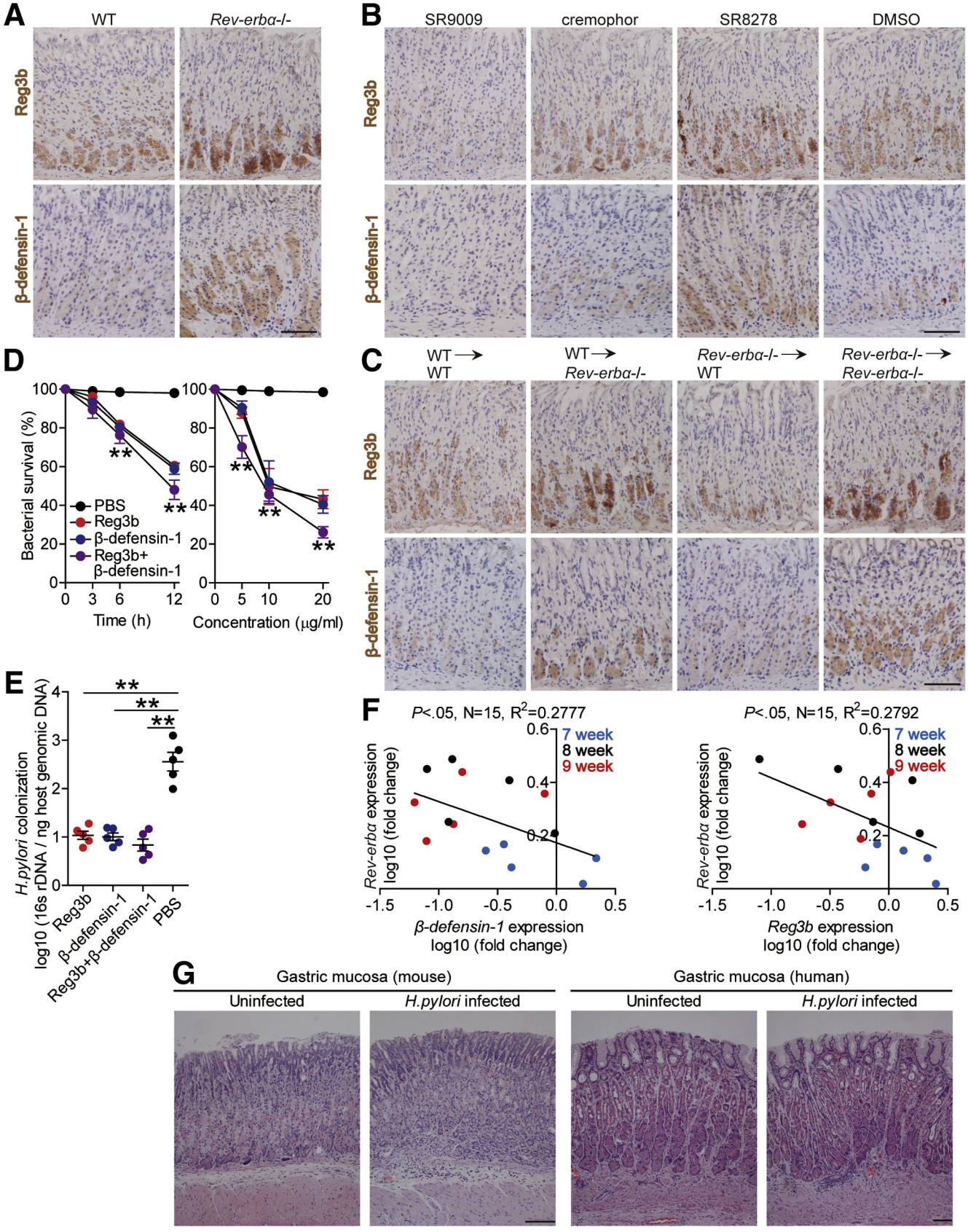
A
WT
Rev-erbα-/-
Reg3b
β-defensin-1
B
SR9009
cremophor
SR8278
DMSO
Reg3b
β-defensin-1
C
WT → WT
WT → Rev-erbα-/-
Rev-erbα-/- → WT
Rev-erbα-/- → Rev-erbα-/-
Reg3b
β-defensin-1
D
Bacterial survival (%)
PBS
Reg3b
β-defensin-1
Reg3b+ β-defensin-1
Time (h)
Concentration (μg/ml)
E
H.pylori colonization log10 (16s rDNA / ng host genomic DNA)
Reg3b
β-defensin-1
Reg3b+β-defensin-1
PBS
F
P<.05, N=15, R2=0.2777
Rev-erbα expression log10 (fold change)
β-defensin-1 expression log10 (fold change)
7 week
8 week
9 week
P<.05, N=15, R2=0.2792
Reg3b expression log10 (fold change)
G
Gastric mucosa (mouse)
Gastric mucosa (human)
Uninfected
H.pylori infected
Uninfected
H.pylori infected

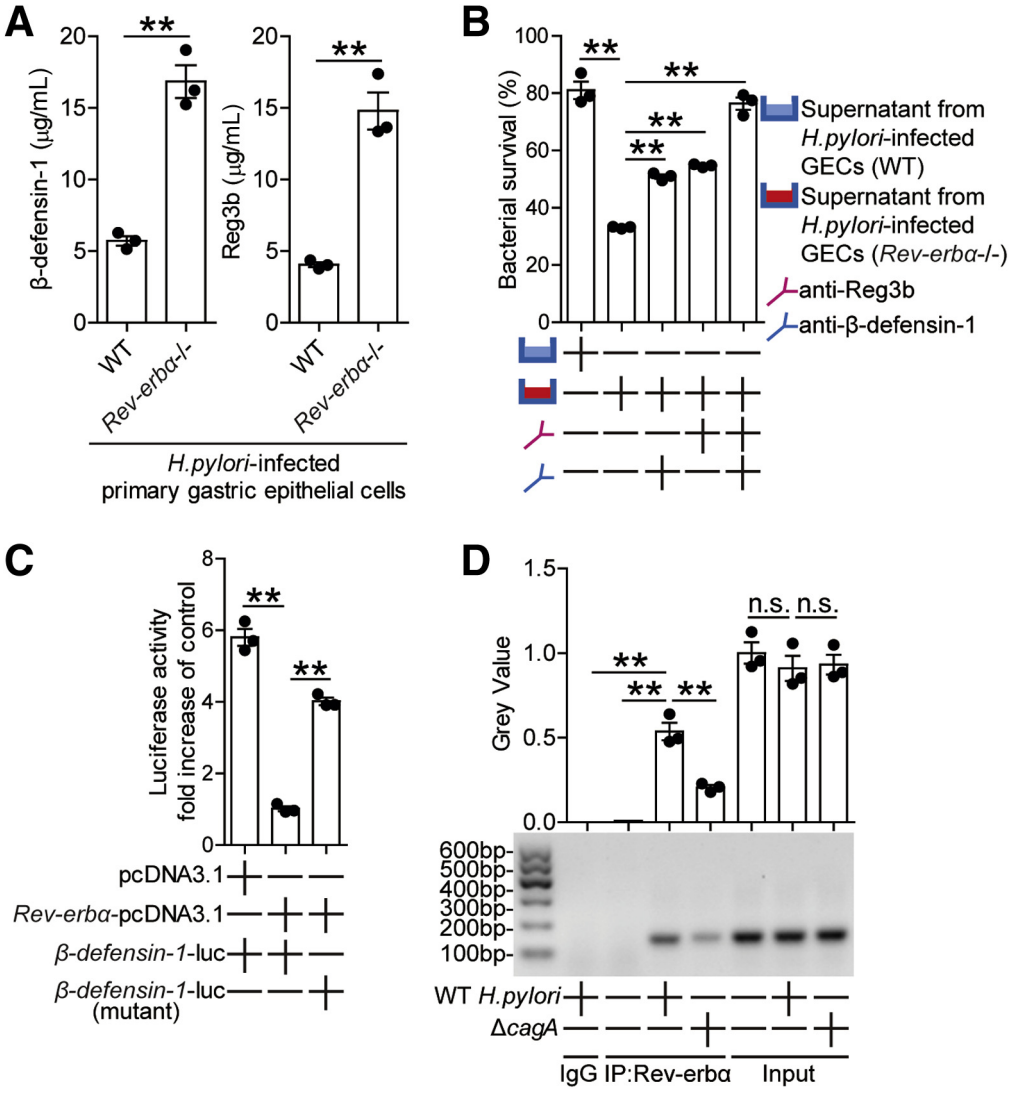

Figure 7. Rev-erbα in GECs inhibits Reg3b and β-defensin-1 directly, which contributes to *H pylori* persistence. (*A*) Primary gastric epithelial cells from uninfected *Rev-erbα*$^{-/-}$ and WT mice were stimulated with WT *H pylori* (MOI = 100) for 24 hours. Reg3b and β-defensin-1 production was measured in cell culture supernatants by ELISA (n = 3). (*B*) In vitro bactericidal assay was performed as described in the Materials and Methods and statistically analyzed (n = 3). (*C*) AGS cells were cotransfected with *β-defensin-1*-luc construct or a mutant construct and *Rev-erbα*-pcDNA3.1 or pcDNA3.1 (control vector) for 48 hours. Luciferase activity was measured to assess β-defensin-1 promoter activity (n = 3). (*D*) Representative data and statistical analysis of chromatin immunoprecipitation assay in AGS cells infected with WT *H pylori* or Δ*cagA*, followed by regular PCR with primers designed for Rev-erbα binding site of β-defensin-1 promoter region (n = 3). ***P* < .01, n.s. *P* > .05 for groups connected by horizontal lines.

Figure 6. (***See previous page***). **Antibacterial proteins Reg3b and β-defensin-1 exerted killing activity against *H pylori* in vitro and in vivo.** (*A–C*) Representative immunohistochemical staining images showing Reg3b or β-defensin-1 expression (brown) in (*A*) gastric mucosa of WT *H pylori*–infected WT and *Rev-erbα*$^{-/-}$ mice, (*B*) gastric mucosa of WT *H pylori*–infected mice injected with Rev-erbα agonist SR9009 or cremophor control, or Rev-erbα antagonist SR8278 or DMSO control, or (*C*) or in gastric mucosa of WT *H pylori*–infected BM chimera mice 8 weeks p.i.. Scale bars: 100 μm. (*D*, *E*) In vitro and in vivo bactericidal assay was performed as described in the Materials and Methods and statistically analyzed (n = 3). (*F*) The correlation between Rev-erbα expression and Reg3b or β-defensin-1 expression in gastric mucosa of WT *H pylori*–infected WT mice 7, 8, and 9 weeks p.i. was analyzed with the Pearson r analyzer (R^2 = 0.2777 and 0.2792, *P* value < .05). (*G*) Representative hematoxylin and eosin staining images showed the histology of gastric mucosa of uninfected and *H pylori*–infected human and mice. Scale bars: 100 μm. ***P* < .01, for groups connected by horizontal lines, or compared with samples treated with PBS.

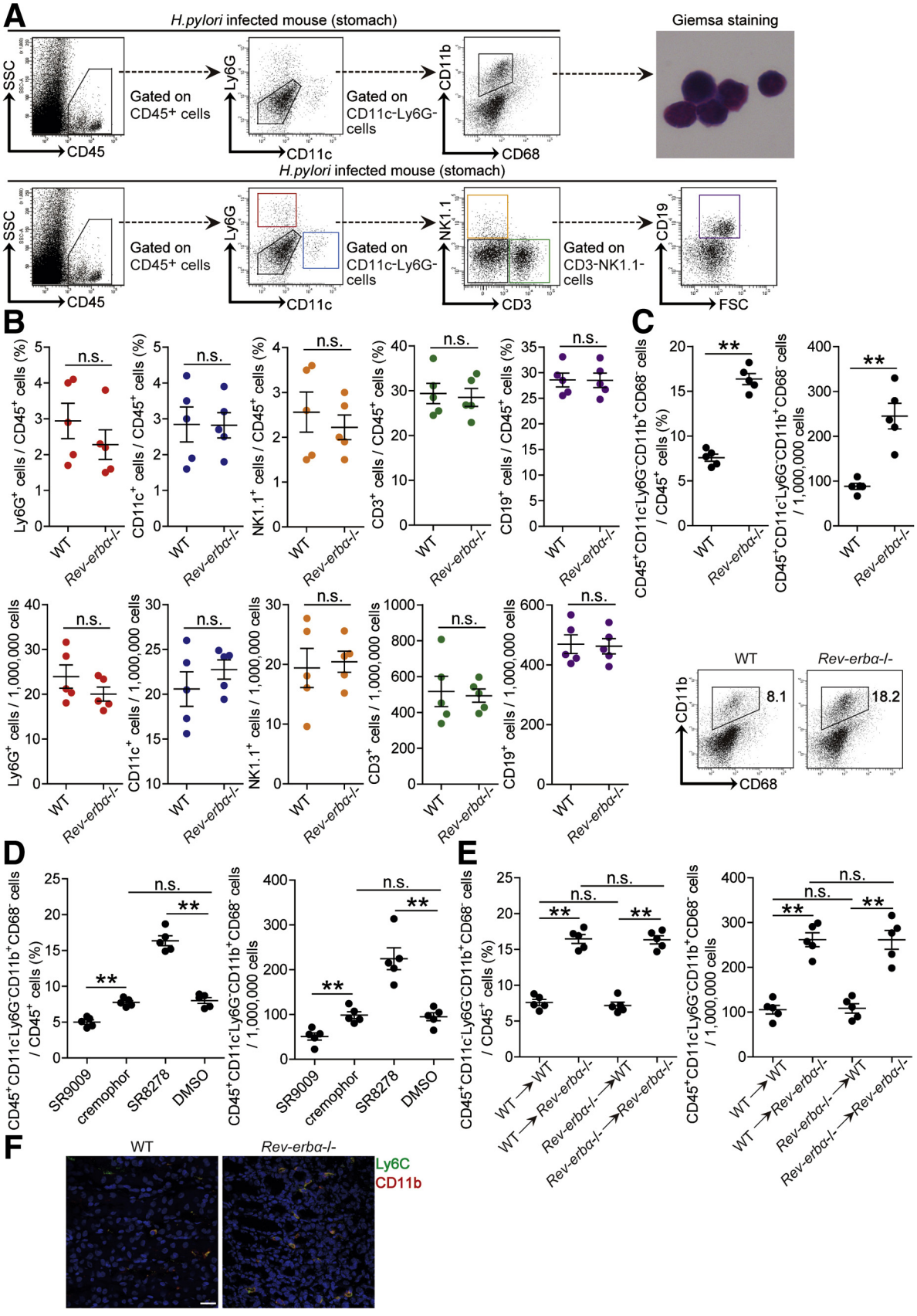
A
H.pylori infected mouse (stomach)
Giemsa staining
SSC
CD45
Gated on CD45+ cells
Ly6G
CD11c
Gated on CD11c-Ly6G- cells
CD11b
CD68
H.pylori infected mouse (stomach)
NK1.1
CD3
Gated on CD3-NK1.1- cells
CD19
FSC
B
C
D
E
F
WT
Rev-erbα-/-
n.s.
**
SR9009
cremophor
SR8278
DMSO
WT→WT
WT→Rev-erbα-/-
Rev-erbα-/-→WT
Rev-erbα-/-→Rev-erbα-/-
8.1
18.2
Ly6C
CD11b

together with the *Rev-erbα*-pcDNA3.1, and retrieved activity when the Rev-erbα binding site on the CCL21 promoter was mutated (Figure 10*G*); further ChIP assays showed that WT *H pylori* infection significantly increased binding activity to the CCL21 promoter by the Rev-erbα Abs (Figure 10*H*), together suggesting that in WT *H pylori*–infected AGS cells, Rev-erbα directly inhibited CCL21 expression. Finally, CCL21 production from AGS cells as well as from mouse primary GECs was negatively regulated in a Rev-erbα–dependent manner (Figure 10*I*). Taken together, our data demonstrate that Rev-erbα inhibits $CD45^+CD11c^-Ly6G^-CD11b^+CD68^-$ myeloid cell accumulation and CCL21 production in gastric mucosa during *H pylori* infection.

Rev-erbα Inhibits $CD45^+CD11c^-Ly6G^-CD11b^+CD68^-$ Myeloid Cell Accumulation In Vivo and Migration In Vitro During H pylori Infection via CCL21-CCR7 Axis

Next, we tried to determine whether $CD45^+CD11c^-Ly6G^-CD11b^+CD68^-$ myeloid cell migration and accumulation during *H pylori* infection was regulated by the Rev-erbα-CCL21 axis. We first showed that $CD45^+CD11c^-Ly6G^-CD11b^+CD68^-$ myeloid cells expressed high levels of the monocyte/macrophage (M)-associated markers Ly6C and F4/80, M1-polarized marker major histocompatibility complex II, and interferon gamma (IFN-γ)–producing T cell function–associated cytokine IL-12, but expressed little M2-polarized markers CD163 and CD206, or monocyte-derived myeloid-derived suppressor cells–associated cytokine IL-10 (Figure 11*A*), and exhibited a monolobar nucleus characteristic of monocyte/macrophage by Giemsa staining (Figure 8*A*). Next, gastric (Figure 11*A*) or blood (Figure 11*B*) $CD45^+CD11c^-Ly6G^-CD11b^+CD68^-$ myeloid cells from *H pylori*–infected humans and mice showed higher expression of CCR7, the chemokine receptor of CCL21. Finally, we conducted a series of loss- and gain-of-function experiments in vivo involving CCL21 or CCR7, and evaluated the $CD45^+CD11c^-Ly6G^-CD11b^+CD68^-$ myeloid cells in gastric mucosa 8 weeks p.i. CCL21 administration significantly increased $CD45^+CD11c^-Ly6G^-CD11b^+CD68^-$ myeloid cell accumulation; conversely, neutralization of CCL21 or CCR7 significantly reduced $CD45^+CD11c^-Ly6G^-CD11b^+CD68^-$ myeloid cell accumulation in gastric mucosa (Figure 11*C*).

To further evaluate the contribution of a Rev-erbα-CCL21-CCR7 axis to the migration of these monocyte-like myeloid cells in vitro, human $CD45^+CD11c^-CD66b^-CD11b^+CD68^-$ myeloid cell chemotaxis assays were performed. It was demonstrated that culture supernatants from *ΔcagA*-infected AGS cells pretreated with nonspecific control small interfering RNA (NC) or from WT *H pylori*–infected AGS cells pretreated with *Rev-erbα* siRNA induced significantly more $CD45^+CD11c^-CD66b^-CD11b^+CD68^-$ myeloid cell migration than those from WT *H pylori*–infected AGS cells pretreated with NC; and this effect was lost upon pretreatment with neutralizing Abs against CCL21 or CCR7 (Figure 11*D*).

Similarly, culture supernatant from *ΔcagA*-infected primary GECs of WT mice or from WT *H pylori*–infected primary GECs of *Rev-erbα*$^{-/-}$ mice also induced significantly more mouse $CD45^+CD11c^-Ly6G^-CD11b^+CD68^-$ myeloid cell migration than those from WT *H pylori*–infected primary GECs of WT mice; and this effect was also lost upon pretreatment with neutralizing Abs against CCL21 or CCR7 (Figure 11*E*). Collectively, these results therefore suggest that a Rev-erbα-CCL21-CCR7 axis contributes to $CD45^+CD11c^-Ly6G^-CD11b^+CD68^-$ myeloid cell accumulation within gastric mucosa during *H pylori* infection.

Rev-erbα Impairs Specific Th1 Cell Response to Promote Bacterial Colonization in Gastric Mucosa During H pylori Infection

Th1 cell response and its effector IFN-γ play key roles in control *H pylori* infection.[19,20] First, there were negative correlations between Rev-erbα and IFN-γ in gastric mucosa of *H pylori*–infected patients and mice (Figure 12*A*), and IFN-γ was increased in gastric mucosa 8 weeks p.i. in *Rev-erbα*$^{-/-}$ mice when compared with that in WT mice (Figure 12*B*). Again, these results were confirmed by our in vivo pharmacological activation or inhibition of Rev-erbα experiments and BM chimera experiments in which non–BM-derived Rev-erbα–expressing cells were largely

Figure 8. (***See previous page***). **Rev-erbα inhibits $CD45^+CD11c^-Ly6G^-CD11b^+CD68^-$ myeloid cell accumulation in gastric mucosa during *H pylori* infection.** (*A*) Representative dot plots of $CD45^+CD11c^+Ly6G^-$ dendritic cells, $CD45^+CD11c^-Ly6G^+$ neutrophils, $CD45^+CD11c^-Ly6G^-CD3^+NK1.1^-$ T cells, $CD45^+CD11c^-Ly6G^-CD3^-NK1.1^+$ natural killer cells, $CD45^+CD11c^-Ly6G^-CD3^-NK1.1^-CD19^+$ B cells, and $CD45^+CD11c^-Ly6G^-CD11b^+CD68^-$ myeloid cells by gating on $CD45^+$ cells in gastric mucosa of WT *H pylori*–infected mice 8 weeks p.i.. Representative Giemsa staining images showing FACS-sorted $CD45^+CD11c^-Ly6G^-CD11b^+CD68^-$ myeloid cells in gastric mucosa of WT *H pylori*–infected WT mice 8 weeks p.i.. (*B*) The levels or numbers of $CD45^+CD11c^+Ly6G^-$ dendritic cells, $CD45^+CD11c^-Ly6G^+$ neutrophils, $CD45^+CD11c^-Ly6G^-CD3^+NK1.1^-$ T cells, $CD45^+CD11c^-Ly6G^-CD3^-NK1.1^+$ natural killer cells, $CD45^+CD11c^-Ly6G^-CD3^-NK1.1^-CD19^+$ B cells, and $CD45^+CD11c^-Ly6G^-CD11b^+CD68^-$ myeloid cells in gastric mucosa of WT *H pylori*–infected WT and *Rev-erbα*$^{-/-}$ mice were compared 8 weeks p.i. (n = 5). (*C–E*) $CD45^+CD11c^-Ly6G^-CD11b^+CD68^-$ myeloid cell levels or $CD45^+CD11c^-Ly6G^-CD11b^+CD68^-$ myeloid cell numbers in (*C*) gastric mucosa of WT *H pylori*–infected WT and *Rev-erbα*$^{-/-}$ mice, (*D*) gastric mucosa of WT *H pylori*–infected mice injected with Rev-erbα agonist SR9009 or cremophor control, or Rev-erbα antagonist SR8278 or DMSO control, or (*E*) gastric mucosa of WT *H pylori*–infected BM chimera mice were compared 8 weeks p.i. (n = 5). (*F*) Representative immunofluorescence staining images showed $Ly6C^+CD11b^+$ myeloid cell infiltration in gastric mucosa of WT *H pylori*–infected WT and *Rev-erbα*$^{-/-}$ mice 8 week p.i.. Scale bars: 20 μm. $^{**}P < .01$, n.s. $P > .05$ for groups connected by horizontal lines.

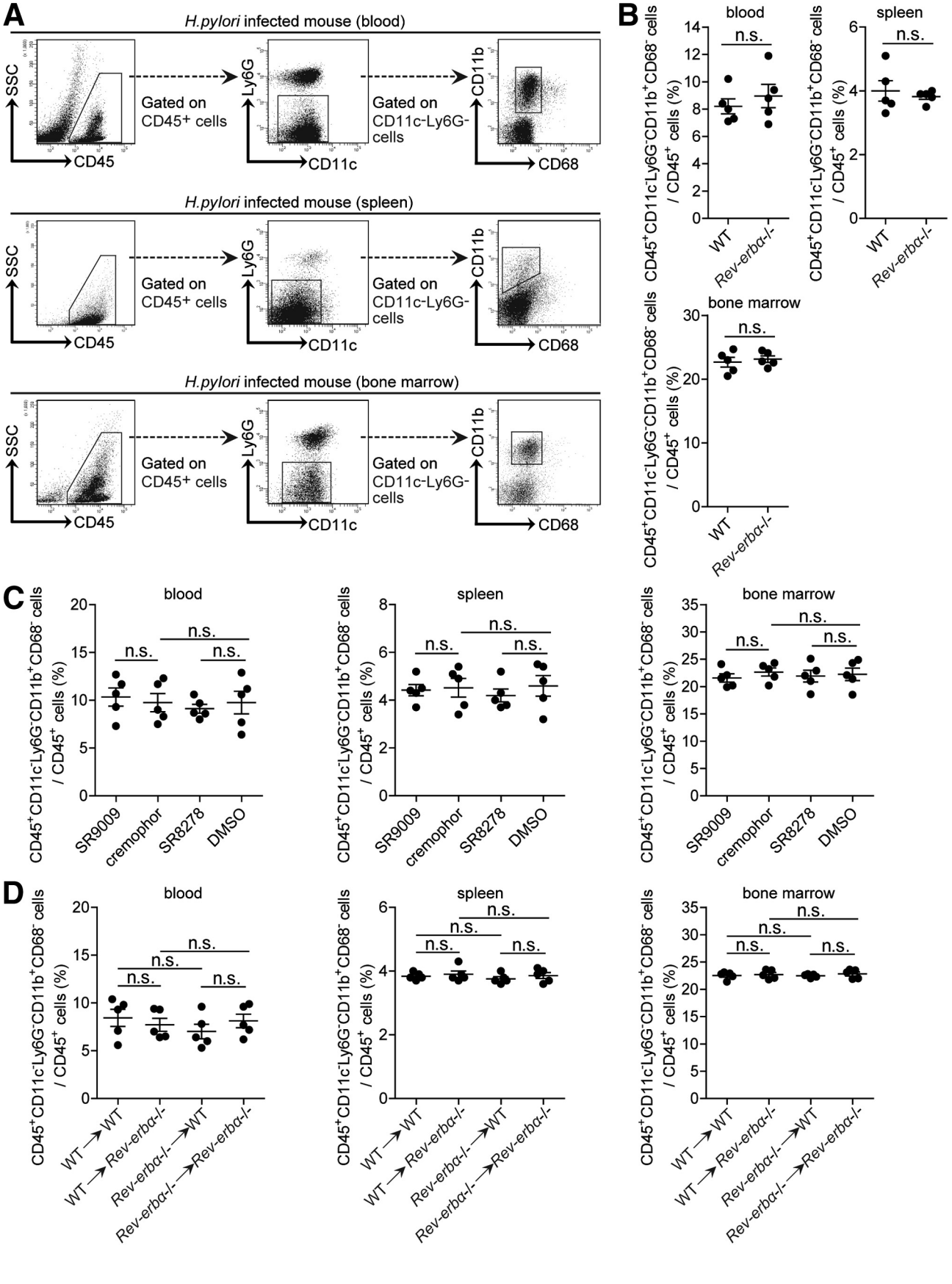
A
H.pylori infected mouse (blood)
SSC
CD45
Gated on CD45+ cells
Ly6G
CD11c
Gated on CD11c-Ly6G- cells
CD11b
CD68
H.pylori infected mouse (spleen)
H.pylori infected mouse (bone marrow)
B
blood
spleen
bone marrow
n.s.
CD45+CD11c-Ly6G-CD11b+CD68- cells / CD45+ cells (%)
WT
Rev-erbα-/-
C
SR9009
cremophor
SR8278
DMSO
D
WT→WT
WT→Rev-erbα-/-
Rev-erbα-/-→WT
Rev-erbα-/-→Rev-erbα-/-

responsible for IFN-γ inhibition in gastric mucosa during *H pylori* infection (Figure 12*C* and *D*). Next, Th1 cell response level was also increased in *Rev-erbα*$^{-/-}$ mice (Figure 12*E*). Notably, myeloid cell/T cell co-cultures showed that gastric CD45^{+}CD11c^{-}Ly6G^{-}CD11b^{+}CD68^{-} myeloid cells from *H pylori*–infected mice induced more Th1 cells from blood or spleen CD4^{+}T cells of *H pylori*–infected mice to proliferate and produce IFN-γ than those from uninfected counterparts (Figure 12*F*), suggesting a promoting effect of CD45^{+}CD11c^{-}Ly6G^{-}CD11b^{+}CD68^{-} myeloid cells on antigen-specific Th1 cell response during *H pylori* infection.

To determine the potential contributions of Rev-erbα–mediated inhibition of specific Th1 cells to *H pylori* colonization, we conducted a series of in vivo adoptive transfer experiments and evaluated bacterial colonization in gastric mucosa 8 weeks p.i. First, CD4^{+} T cells from *H pylori*–infected WT donors into WT recipients effectively reduced *H pylori* colonization when compared with WT mice received CD4^{+} T cells from uninfected WT donors, suggesting specific CD4^{+} T cells contribute to reduced bacterial colonization (Figure 12*G*). Next, transferring CD4^{+} T cells from *H pylori*–infected WT donors into uninfected (or naïve) *Rev-erbα*$^{-/-}$ recipients effectively reduced *H pylori* colonization when compared with those in the uninfected WT mice received the same CD4^{+} T cells, suggesting Rev-erbα–mediated inhibition on *H pylori*–specific CD4^{+} T cells leading to increased bacterial colonization (Figure 12*G*). Finally, transferring CD4^{+} T cells from *H pylori*–infected WT donors into uninfected *Rev-erbα*$^{-/-}$ recipients effectively reduced *H pylori* colonization when compared with those in the uninfected *Rev-erbα*$^{-/-}$ recipients received CD4^{+} T cells from *H pylori*–infected *IFN-γ*$^{-/-}$ donors, suggesting Rev-erbα–mediated inhibition on IFN-γ production of *H pylori*–specific CD4^{+} T cells (Th1 cells) leading to increased bacterial colonization (Figure 12*G*), which was also reflected by increased colonization in *IFN-γ*$^{-/-}$ mice (Figure 12*H*). Overall, these results indicate that Rev-erbα promotes gastric *H pylori* colonization, most likely through inhibiting *H pylori*–specific Th1 cells' IFN-γ response.

Discussion

Our results from both in vivo and in vitro gain- and loss-of-function experiments identify Rev-erbα as a pathological regulator that benefits bacterial colonization and contributes to gastric *H pylori* persistence. This is supported by several observations. First, Rev-erbα is preferentially expressed in GECs during *H pylori* infection, such as gastric pepsinogen II^{+} cells, and *Rev-erbα*$^{-/-}$ mice have notably decreased *H pylori* colonization associated with a marked increase in antibacterial protein content, chemokine production and Th1 cell response within gastric mucosa. We observed similar alterations upon knocking down Rev-erbα in AGS cells (higher Reg3b and β-defensin-1 content and impaired CCL21-derived chemotaxis function). By contrast, pharmacological activation of Rev-erbα in vivo in mice infected with *H pylori* and in vitro in *H pylori*–infected AGS cells resulted in the opposite phenotype, highlighting direct Rev-erbα effect on GECs. Second, our data indicate that *H pylori* induces Rev-erbα expression in GECs through the ERK-NF-κB signaling pathway, and that *H pylori* virulence factor *cagA* plays an essential role in this process. Finally, we show that GEC Rev-erbα regulates several genes involved in different steps of the host defense process, including genes more specifically dedicated to innate (*Reg3b* and *β-defensin-1*) and adaptive defense (*CCL21* and *IFN-γ*). Together, these data support the concept that Rev-erbα acts through a two-pronged mechanism, involving both suppression of host innate defense and inhibition of host adaptive defense. Thus, during *H pylori* infection, when Rev-erbα is induced, there is a progressive impaired host defense within gastric mucosa, allowing for gastric *H pylori* persistence. And the role of Rev-erbα during *H pylori*–associated carcinogenesis process needs further investigation.

In this study, we not only identified a previously unrecognized role for Rev-erbα during *H pylori* infection, but also found that Rev-erbα expression was readily induced upon *H pylori* infection ex vivo in primary gastric tissues. This response is consistent with previous observations on Rev-erbα expression in inflamed tissues, such as liver[21] and skeletal muscle.[22] The regulation of Rev-erbα by *H pylori* provides a molecular mechanism whereby *H pylori* controls Rev-erbα expression through its virulence factor *cagA*. The *cagA* is crucial in the pathogenicity of *H pylori* that is injected into GECs via the type IV secretion system (T4SS) to modulate the phenotype and function of GECs.[14] Lack of *cagA* activity in *H pylori* is associated with impaired expression of Rev-erbα in GECs, attenuated inhibition of Rev-erbα–mediated CCL21 expression and decreased CD45^{+}CD11c^{-}Ly6G^{-}CD11b^{+}CD68^{-} myeloid cell chemotaxis. Thus, our findings that *H pylori*–associated virulence factor *cagA* was necessary to induce maximal Rev-erbα expression may suggest that intrinsic factors encoded by the infection itself are likely to be important in influencing the role of Rev-erbα. In addition, we revealed that ERK pathway activation–mediated *Rev-erbα* promoter transcription initiation is essential for the induction of Rev-erbα in GECs in response to *H pylori*. Of note, it is reported that several inflammatory factors such as TGF-β[23] and transcription factors such as NF-κB[24] are involved in Rev-erbα induction in hepatic stellate cells or under oxidative stress, which

Figure 9. (***See previous page***). **Rev-erbα has no effects on blood, spleen, or BM CD45^{+}CD11c^{-}Ly6G^{-}CD11b^{+}CD68^{-} myeloid cells during *H pylori* infection.** (*A*) Representative dot plots of CD45^{+}CD11c^{-}Ly6G^{-}CD11b^{+}CD68^{-} myeloid cells by gating on CD45^{+} cells in peripheral blood, spleen or BM of WT *H pylori*–infected WT mice 8 weeks p.i.. (*B–D*) The levels of CD45^{+}CD11c^{-}Ly6G^{-}CD11b^{+}CD68^{-} myeloid cells in (*B*) peripheral blood, spleen, or BM of WT *H pylori*–infected WT and *Rev-erbα*$^{-/-}$ mice; (*C*) gastric mucosa of WT *H pylori*–infected mice injected with Rev-erbα agonist SR9009 or cremophor control, or Rev-erbα antagonist SR8278 or DMSO control; or (*D*) gastric mucosa of WT *H pylori*–infected BM chimera mice were compared 8 weeks p.i. (n = 5). n.s. $P > .05$ for groups connected by horizontal lines.

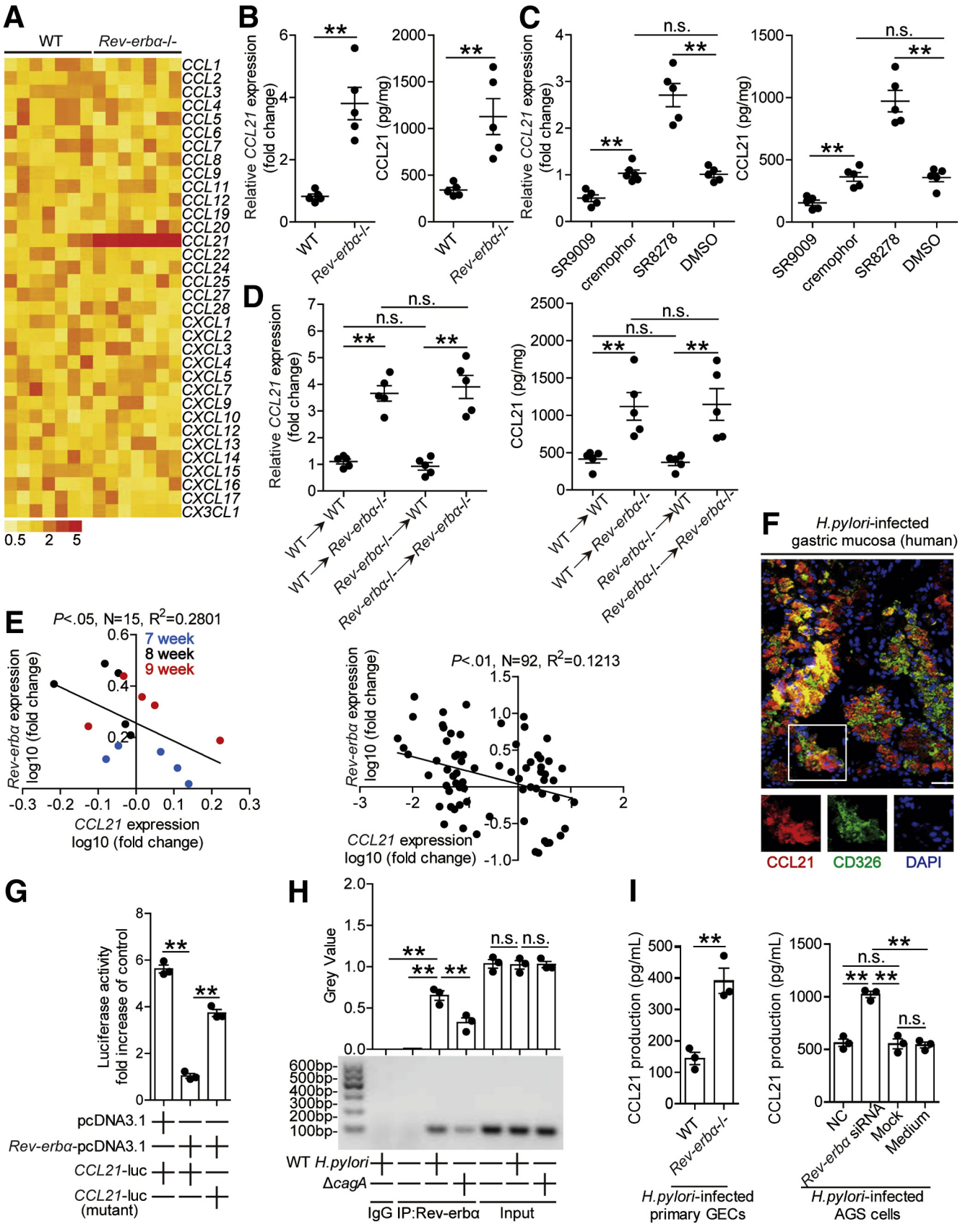
A
WT
Rev-erbα-/-
CCL1
CCL2
CCL3
CCL4
CCL5
CCL6
CCL7
CCL8
CCL9
CCL11
CCL12
CCL19
CCL20
CCL21
CCL22
CCL24
CCL25
CCL27
CCL28
CXCL1
CXCL2
CXCL3
CXCL4
CXCL5
CXCL7
CXCL9
CXCL10
CXCL12
CXCL13
CXCL14
CXCL15
CXCL16
CXCL17
CX3CL1
0.5 2 5
B
Relative CCL21 expression (fold change)
CCL21 (pg/mg)
WT
Rev-erbα-/-
C
Relative CCL21 expression (fold change)
CCL21 (pg/mg)
n.s.
SR9009
cremophor
SR8278
DMSO
D
Relative CCL21 expression (fold change)
CCL21 (pg/mg)
n.s.
WT → WT
WT → Rev-erbα-/-
Rev-erbα-/- → WT
Rev-erbα-/- → Rev-erbα-/-
E
P<.05, N=15, R2=0.2801
7 week
8 week
9 week
Rev-erbα expression log10 (fold change)
CCL21 expression log10 (fold change)
P<.01, N=92, R2=0.1213
Rev-erbα expression log10 (fold change)
CCL21 expression log10 (fold change)
F
H.pylori-infected gastric mucosa (human)
CCL21
CD326
DAPI
G
Luciferase activity fold increase of control
pcDNA3.1
Rev-erbα-pcDNA3.1
CCL21-luc
CCL21-luc (mutant)
H
Grey Value
n.s.
600bp-
500bp-
400bp-
300bp-
200bp-
100bp-
WT H.pylori
ΔcagA
IgG
IP:Rev-erbα
Input
I
CCL21 production (pg/mL)
WT
Rev-erbα-/-
H.pylori-infected primary GECs
n.s.
NC
Rev-erbα siRNA
Mock
Medium
H.pylori-infected AGS cells

resembles our data on Rev-erbα regulation by NF-κB in *H pylori*–infected GECs.

Host defense is a dynamic host-pathogen interaction process that ensures the selective clearance of invading pathogens, which is particularly important in infected cells such as GECs. It has been reported that Rev-erbα ameliorates *Mycobacterium tuberculosis* clearance through regulating autophagy-related genes,[11] whereas our data demonstrate that Rev-erbα impedes *H pylori* clearance by regulating several genes involved in innate and adaptive defense. Several antibacterial proteins including LL-37[25] and β-defensin-2[17] exerts antimicrobial activity against *H pylori*, here we add Reg3b and β-defensin-1 onto that list which are selectively suppressed by *H pylori*–induced Rev-erbα[26] that represses *β-defensin-1* gene directly triggering decreased bactericidal effect against *H pylori* to maintain gastric bacterial persistence. Several data have shown that Rev-erbα represses many cytokine and chemokine gene expression such as IL-6,[27] IL-17,[28] and CCL2[29] in inflammatory diseases. In our model, Rev-erbα downregulates CCL21 expression, leading to impaired chemotaxis of $CD45^+CD11c^-Ly6G^-CD11b^+CD68^-$ myeloid cells and therefore decreased stimulation on *H pylori*–specific Th1 cells. IFN-γ, one of the key effector molecules of the Th1 cells, is reported to play key roles in controlling *H pylori* infection in mice[19] and humans.[30] Moreover, IFN-γ deficiency indeed results in uncontrolled colonization of *H pylori* in gastric mucosa.[20] Notably, our findings mechanistically demonstrate for the first time that *H pylori*–induced Rev-erbα in GECs impairs host *H pylori*–specific Th1 response resulting in increased bacterial colonization. Together, these data support a prominent role for Rev-erbα in *H pylori* infection on connecting innate and adaptive host defense. Given the apparent relationship between Rev-erbα levels and the extent of bacterial colonization in *H pylori*–infected patients observed in this study, Rev-erbα should be considered as a novel diagnostic biomarker for *H pylori* infection–associated diseases. Specifically, our in vitro and in vivo data together provide a multistep model of *H pylori* persistent infection involving direct and indirect interactions among *H pylori*, GECs, Rev-erbα, Reg3b, β-defensin-1, CCL21, $CD45^+CD11c^-Ly6G^-CD11b^+CD68^-$ myeloid cells, and Th1 cells within the gastric mucosa (Figure 13).

Although eradication therapy for *H pylori* by oral antibiotics progressed in recent years,[31,32] it is noteworthy that *H pylori* colonization commonly persists because of increased antimicrobial resistance and impaired host defense. In this regard, our findings suggest a possible therapeutic target, Rev-erbα, for decreasing gastric *H pylori* persistence. In addition to the direct action of Rev-erbα on genes associated with host defense, Rev-erbα deletion, or overexpression causes disturbed circadian rhythmicity[33] may contribute to the observed phenotype. In conclusion, Rev-erbα is a novel pathological regulator of the function of host defense during *H pylori* infection. Thus, pharmacological inhibition of Rev-erbα may be a promising approach for the treatment of gastric diseases caused by *H pylori* infection.

Materials and Methods

Patients and Specimens

The gastric biopsy specimens and blood were collected from 92 *H pylori*–infected and 32 uninfected patients who underwent upper esophagogastroduodenoscopy for dyspeptic symptoms at XinQiao Hospital (Table 1). *H pylori* infection was determined by [^{14}C] urea breath test and rapid urease test of biopsy specimens taken from the antrum, and subsequently conformed by real-time polymerase chain reaction (PCR) for 16s recombinant DNA (rDNA) and serology test for specific anti-*H pylori* Abs.[34] For isolation of human primary GECs, fresh non-tumor gastric tissues (at least 5 cm distant from the tumor site) were obtained from gastric cancer patients who underwent surgical resection and were determined as *H pylori*–negative individuals (conformed by real-time PCR for 16s rDNA and serology test for specific anti-*H pylori* Abs) as previous at the Southwest Hospital. None of these patients had received chemotherapy or radiotherapy before sampling. Individuals with atrophic gastritis, hypochlorhydria, antibiotics treatment, autoimmune disease, infectious diseases and multiprimary cancer were excluded. The study was approved by the Ethics Committee of XinQiao Hospital and Southwest Hospital of Third Military Medical University. A written informed consent was obtained from each subject.

Figure 10. (*See previous page*). Rev-erbα inhibits CCL21 in gastric mucosa during *H pylori* infection. (*A*) The mRNA expression profiles of chemokines in gastric mucosa of WT *H pylori*–infected WT and *Rev-erbα*$^{-/-}$ mice 8 weeks p.i. was analyzed by real-time PCR (n = 5). (*B–D*) The mRNA expression or the concentrations of CCL21 in (*B*) gastric mucosa of WT *H pylori*–infected WT and *Rev-erbα*$^{-/-}$ mice, (*C*) gastric mucosa of WT *H pylori*–infected mice injected with Rev-erbα agonist SR9009 or cremophor control, or Rev-erbα antagonist SR8278 or DMSO control, or (*D*) gastric mucosa of WT *H pylori*–infected BM chimera mice were compared 8 weeks p.i. (n = 5). (*E*) The correlation between Rev-erbα expression and CCL21 expression in gastric mucosa of WT *H pylori*–infected WT mice 7, 8, and 9 weeks p.i. or in gastric mucosa of *H pylori*–infected patients was analyzed. (*F*) Representative immunofluorescence staining images showing CCL21-expressing (red) $CD326^+$ cells (green) in gastric mucosa of *H pylori*–infected patients. Scale bars: 20 μm. (*G*) AGS cells were cotransfected with *CCL21*-luc construct or a mutant construct and *Rev-erbα*-pcDNA3.1 or pcDNA3.1 (control vector) for 48 hours. Luciferase activity was measured to assess CCL21 promoter activity (n = 3). (*H*) Representative data and statistical analysis of chromatin immunoprecipitation assay in AGS cells infected with WT *H pylori* or Δ*cagA*, followed by regular PCR with primers designed for Rev-erbα binding site of CCL21 promoter region (n = 3). (*I*) Primary GECs from uninfected *Rev-erbα*$^{-/-}$ and WT mice, and Rev-erbα siRNA, NC, or lipo2000-only (Mock) pretreated AGS cells or AGS cells without treatment (medium) were infected with WT *H pylori* (MOI = 100) for 24 hours. CCL21 production was measured in cell culture supernatants by ELISA (n = 3). $^{**}P < .01$, n.s. $P > .05$ for groups connected by horizontal lines.

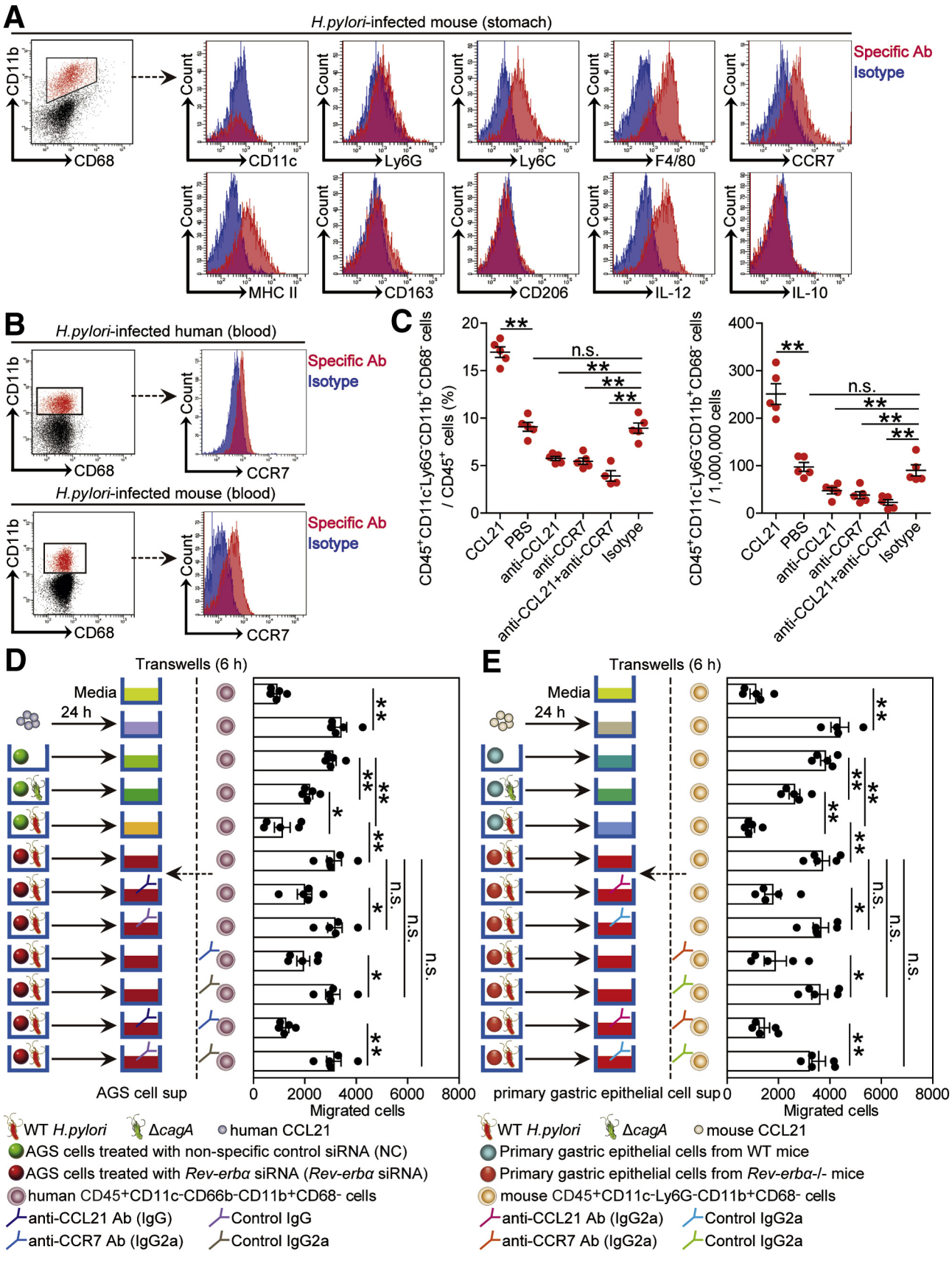
A
H.pylori-infected mouse (stomach)
CD11b
CD68
Count
CD11c
Ly6G
Ly6C
F4/80
CCR7
MHC II
CD163
CD206
IL-12
IL-10
Specific Ab
Isotype
B
H.pylori-infected human (blood)
H.pylori-infected mouse (blood)
C
CD45+CD11c-Ly6G-CD11b+CD68- cells / CD45+ cells (%)
CD45+CD11c-Ly6G-CD11b+CD68- cells / 1,000,000 cells
CCL21
PBS
anti-CCL21
anti-CCR7
anti-CCL21+anti-CCR7
Isotype
n.s.
D
Transwells (6 h)
Media
24 h
AGS cell sup
Migrated cells
E
primary gastric epithelial cell sup
WT H.pylori
ΔcagA
human CCL21
mouse CCL21
AGS cells treated with non-specific control siRNA (NC)
AGS cells treated with Rev-erba siRNA (Rev-erba siRNA)
Primary gastric epithelial cells from WT mice
Primary gastric epithelial cells from Rev-erbα-/- mice
human CD45+CD11c-CD66b-CD11b+CD68- cells
mouse CD45+CD11c-Ly6G-CD11b+CD68- cells
anti-CCL21 Ab (IgG)
Control IgG
anti-CCR7 Ab (IgG2a)
Control IgG2a

Antibodies and Other Reagents

For information on antibodies and other reagents, see Table 2.

Mice

All breeding and experiments were undertaken with review and approval from the Animal Ethical and Experimental Committee of Third Military Medical University. C57BL/6 *Rev-erbα*$^{+/-}$ mice were obtained from the Jackson Laboratory (Bar Harbor, ME). C57BL/6 *Rev-erbα*$^{-/-}$ mice and their littermate control (WT) mice were generated by breeding between C57BL/6 *Rev-erbα*$^{+/-}$ mice. C57BL/6 *interferon-γ*$^{-/-}$ (*IFN-γ*$^{-/-}$) mice were kindly provided by Dr. Richard A. Flavell (Yale University). All mice used in experiments were viral Ab negative for pathogenic murine viruses, negative for pathogenic bacteria including *Helicobacter* spp. and parasites, and were maintained under specific pathogen–free conditions in a barrier sustained facility and provided with sterile food and water.

Bacteria Culture and Infection of Mice With Bacteria

H pylori NCTC 11637 (*cagA* positive) (WT *H pylori*) and *cagA*-knockout mutant *H pylori* NCTC 11637 (*ΔcagA*) or *H pylori* 26695 were grown in brain-heart infusion plates containing 10% rabbit blood at 37°C under microaerophilic conditions. For infecting mouse, bacteria were propagated in Brucella broth with 5% fetal bovine serum (FBS) with gentle shaking at 37°C under microaerobic conditions. After culture for 1 day, live bacteria were collected and adjusted to 10^9 colony-forming units (CFU)/mL. The mice were fasted overnight and orogastrically inoculated twice at a 1-day interval with 3×10^8 CFU bacteria. *H pylori* infection status and *H pylori*–induced gastritis in murine experiments were confirmed using real-time PCR of *H pylori* 16s rDNA, urease biopsy assays, Warthin-Starry staining, and immunohistochemical staining for *H pylori*.[34,35]

Generation of BM Chimera Mice

The following BM chimeric mice were created: male WT BM → female WT mice, male WT BM → female *Rev-erbα*$^{-/-}$ mice, male *Rev-erbα*$^{-/-}$ BM → female WT mice, and male *Rev-erbα*$^{-/-}$ BM → female *Rev-erbα*$^{-/-}$ mice. BM cells were collected from the femurs and tibia of donor mice by aspiration and flushing, and were suspended in phosphate-buffered saline (PBS) at the concentration of 5×10^7/mL. The BM in recipient mice was ablated with lethal irradiation (8 Gy). Then, the animals received intravenously 1.5×10^7 BM cells from donor mice in a volume of 300 μL sterile PBS under the anesthesia. Thereafter, the transplanted BM was allowed to reconstitute for 8 weeks before subsequent experimental procedures. To verify successful engraftment and reconstitution of the BM in the host mice, genomic DNA was isolated from tail tissues of each chimera mouse 8 weeks after BM transplantation. Quantitative PCR was performed to detect the *Sry* gene present in the Y chromosome (primers seen in Table 3) and mouse β2-microglobulin gene as an internal control. The chimeric rates were calculated on the assumption that the ratio of the Sry to β2-microglobulin gene was 100% in male mice. We confirmed that the chimeric rates were consistently higher than 90%. After BM reconstitution was confirmed, mice were infected with bacteria as described previously.

Antibodies/CCL21/Reg3b/β-Defensin-1/Rev-erbα Agonist/Rev-erbα Antagonist Administration

One day after infection with WT *H pylori* as described previously, WT mice were injected intraperitoneally with recombinant mouse CCL21 (25 μg) or Reg3b or β-defensin-1 (50 μg), or anti-mouse CCL21 or anti-mouse CCR7 or isotype control Abs (100 μg), or Rev-erbα agonist SR9009 (100 mg/kg, dissolved in cremophor) or cremophor control, or Rev-erbα antagonist SR8278 (25 mg/kg, dissolved in dimethyl sulfoxide [DMSO]) or DMSO control and repeated every week until the mice were sacrificed.

T Cell Adoptive Transfer

One day before infection with WT *H pylori*, WT or *Rev-erbα*$^{-/-}$ mice were injected intravenously (1×10^6 cells/mouse) with purified spleen CD4$^+$ T cells (StemCell Technologies, Vancouver, Canada) from uninfected WT mice, or WT *H pylori*–infected WT mice or WT *H pylori*–infected *IFN-γ*$^{-/-}$ mice (8 week p.i.). Then, the recipient mice were infected with bacteria as described previously and sacrificed for bacteria colonization evaluation at week 8 p.i..

Evaluation of Bacteria Colonization

The mice were sacrificed at the indicated time points. The stomach was cut open from the greater curvature and

Figure 11. (***See previous page***). **Rev-erbα inhibits CD45$^+$CD11c$^-$Ly6G$^-$CD11b$^+$CD68$^-$ myeloid cell accumulation in vivo and migration in vitro during *H pylori* infection via CCL21-CCR7 axis.** (*A*) Expression of CD11c, Ly6G, Ly6C, F4/80, CCR7, MHC II, CD163, CD206, IL-12, and IL-10 on/in gastric CD45$^+$CD11c$^-$Ly6G$^-$CD11b$^+$CD68$^-$ myeloid cells from WT *H pylori*–infected WT mice 8 weeks p.i.. Red histograms represent staining of the molecules of interest; blue histograms represent isotype control. (*B*) Representative dot plots of CCR7 expression on blood CD45$^+$CD11c$^-$CD66b$^-$CD11b$^+$CD68$^-$ myeloid cells in blood of *H pylori*–infected patients or CCR7 expression on CD45$^+$CD11c$^-$Ly6G$^-$CD11b$^+$CD68$^-$ myeloid cells of WT *H pylori*–infected mice 8 weeks p.i.. (*C*) CD45$^+$CD11c$^-$Ly6G$^-$CD11b$^+$CD68$^-$ myeloid cell levels or numbers in gastric mucosa of WT *H pylori*–infected mice injected with CCL21 or PBS control, or Abs against CCL21 or CCR7 or corresponding isotype control Ab were compared 8 weeks p.i. (n = 5). (*D*, *E*) Human CD45$^+$CD11c$^-$CD66b$^-$CD11b$^+$CD68$^-$ myeloid cell migration and mouse CD45$^+$CD11c$^-$Ly6G$^-$CD11b$^+$CD68$^-$ myeloid cell migration were assessed via a transwell assays as described in the Materials and Methods and statistically analyzed (n = 5). *$P < .05$, **$P < .01$, n.s. $P > .05$ for groups connected by horizontal lines.

half of the tissue was cut into 4 parts for RNA extraction, DNA extraction, protein extraction, and tissue fixation for immunohistochemistry or immunofluorescence staining, respectively. DNA of the biopsy specimens were extracted with QIAamp DNA Mini Kit (Qiagen, Hilden, Germany). As previously described,[36] *H pylori* colonization was quantified by measuring *H pylori*–specific 16s rDNA using specific primer and probe (Table 3) by the TaqMan method. The amount of mouse β2-microglobulin DNA in the same specimen was used to normalize the data. According to a previous study,[37] the density of *H pylori* was shown as the number of bacterial genomes per nanogram of host genomic DNA. Another half of stomach was used for isolation of single cells as described subsequently. The isolated single

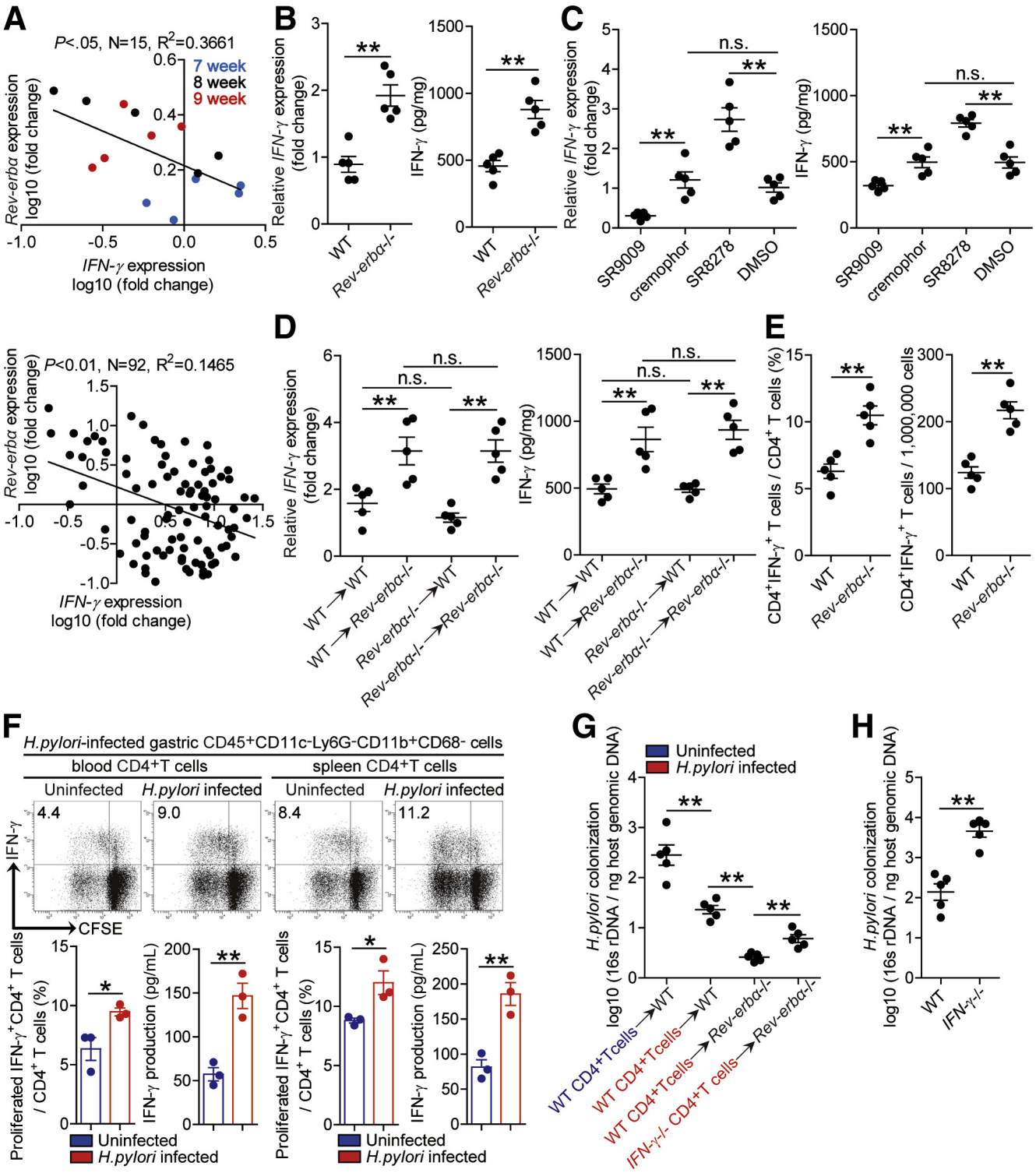

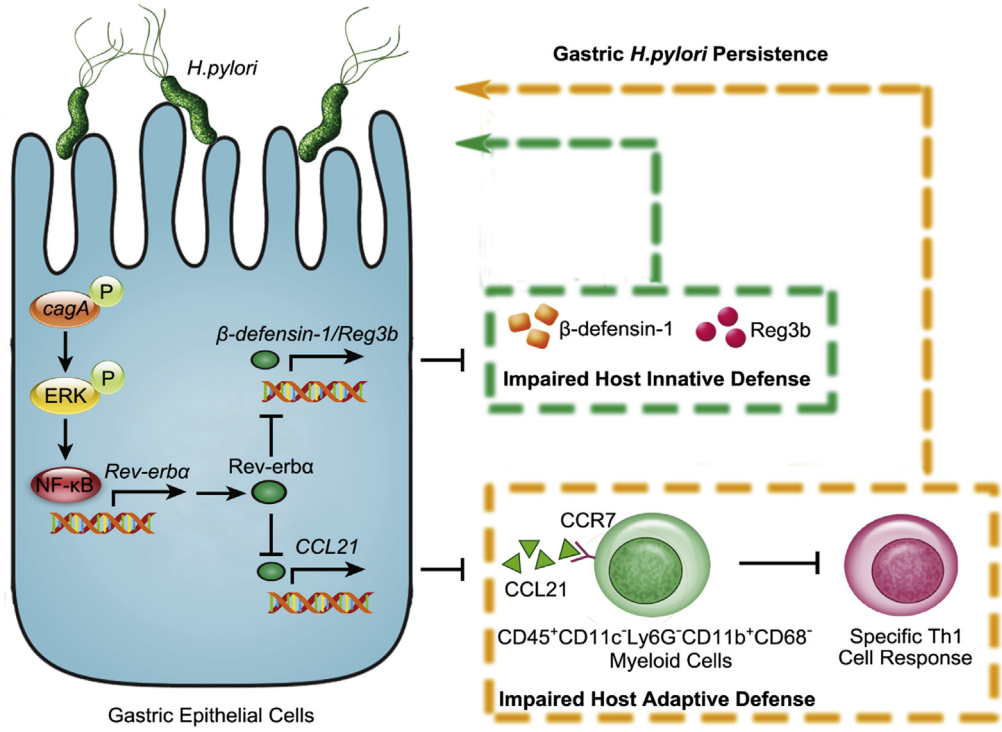

Figure 13. A proposed model of crosstalk among *H pylori*, GECs, Rev-erbα, Reg3b, β-defensin-1, CCL21, $CD45^+CD11c^-Ly6G^-CD11b^+CD68^-$ myeloid cells, and Th1 cell response leading to Rev-erbα-mediated procolonization in gastric mucosa during *H pylori* infection.

cells were collected and analyzed by flow cytometry staining.

Isolation of Single Cells From Tissues

Fresh tissues were washed three times with Hank's solution containing 1% FBS, cut into small pieces, collected in RPMI 1640 containing 1 mg/mL collagenase IV and 10 mg/mL DNase I, and then mechanically dissociated by using the gentle MACS Dissociator (Miltenyi Biotec, Bergisch Gladbach, Germany). Dissociated cells were further incubated for 0.5–1 hour at 37°C under continuous rotation. The cell suspensions were then filtered through a 70-μm cell strainer (BD Labware; Becton Dickinson, Franklin Lakes, NJ).

Cell/Tissue Culture, Transfection, and Stimulation

Primary GECs were purified from gastric tissue single-cell suspensions from uninfected donors or mice with a MACS column purification system using anti-human or mouse CD326 magnetic beads. The sorted primary GECs were used only when their viability was determined >90% and their purity was determined >95%. For human GEC lines (AGS cells, GES-1 cells, HGC-27 cells, SGC-7901 cells, BGC-823 cells), 3×10^5 cells per well in 12-well cell culture plate (for real-time PCR) or 1×10^6 cells per well in 6-well cell culture plate (for Western blot and enzyme-linked immunosorbent assay [ELISA]) were starved in Dulbecco's modified Eagle medium/F-12 medium supplemented with penicillin (100 U/mL) and streptomycin (100 μg/mL) for 6 hours in a humidified environment containing 5% CO_2 at

Figure 12. (***See previous page***). **Rev-erbα impairs specific Th1 cell response to promote bacterial colonization in gastric mucosa during *H pylori* infection.** (*A*) The correlation between Rev-erbα expression and IFN-γ expression in gastric mucosa of WT *H pylori*–infected WT mice 7, 8, and 9 weeks p.i. or in gastric mucosa of *H pylori*–infected patients was analyzed with the Pearson r analyze ($R^2 = 0.3661$ and 0.1485, *P* value < .05 and < .01). (*B–D*) The mRNA expression and the concentrations of IFN-γ in (*B*) gastric mucosa of WT *H pylori*–infected WT and *Rev-erbα*$^{-/-}$ mice, (*C*) gastric mucosa of WT *H pylori*–infected mice injected with Rev-erbα agonist SR9009 or cremophor control, or Rev-erbα antagonist SR8278 or DMSO control, or (*D*) gastric mucosa of WT *H pylori*–infected BM chimera mice were compared 8 weeks p.i. (n = 5). (*E*) $CD4^+IFN\text{-}\gamma^+$ T cell levels or numbers in gastric mucosa of WT *H pylori*–infected WT and *Rev-erbα*$^{-/-}$ mice were compared 8 weeks p.i. (n = 5). (*F*) Carboxyfluorescein succinimidyl ester (CFSE)–labeled peripheral or spleen $CD4^+$ T cells from uninfected or WT *H pylori*–infected mice (8 weeks p.i.) were co-cultured for 5 days with FACS-sorted gastric $CD45^+CD11c^-Ly6G^-CD11b^+CD68^-$ myeloid cells from WT *H pylori*–infected mice (8 weeks p.i.). Representative data and statistical analysis of $CD4^+IFN\text{-}\gamma^+$ T cell level and IFN-γ production were shown (n = 3). (*G*) The bacteria colonization in gastric mucosa of WT *H pylori*–infected WT and *Rev-erbα*$^{-/-}$ mice adoptively transferred with spleen $CD4^+$ T cells from uninfected or WT *H pylori*–infected WT or *IFN-γ*$^{-/-}$ mice (8 weeks p.i.) was compared 8 weeks p.i. (n = 5). (*H*) The bacteria colonization in gastric mucosa of WT *H pylori*–infected WT and *IFN-γ*$^{-/-}$ mice was compared 8 weeks p.i. (n = 5). **P* < .05, ***P* < .01, n.s. *P* > .05 for groups connected by horizontal lines.

Table 1. Clinical Characteristics of Patients

Variables	*H pylori* Infected	Uninfected
Age, y	46 (21–73)	45 (24–68)
Male/female	53/39	18/14

NOTE. Values are median (interquartile range) or n. Exclusion criteria were previous treatment for *H pylori* infection, use of inhibitors of acid secretion or antibiotics during the 2 months before the study, use of anticoagulant drugs in the last week, gastrointestinal malignancy, severe concomitant cardiovascular, respiratory or endocrine diseases, clinically significant renal or hepatic disease, hematological disorders, previous gastroesophageal surgery, history of allergy to any of the drug used in the study, pregnancy or lactation, alcohol abuse, drug addiction, severe neurological or psychiatric disorders, and long-term use of corticosteroids or anti-inflammatory drugs.

37 °C. Then the cells were incubated in antibiotic-free Dulbecco's modified Eagle medium/F-12 medium supplemented with 10% FBS instead. The cell lines were used when their viability was determined >90%. Human GEC lines, primary GECs, or primary gastric mucosa tissues from uninfected donors or mice were infected with WT *H pylori*, *ΔcagA* or *H pylori* 26695 at a multiplicity of infection (MOI) of 100 for 24 hours. AGS cells were also infected with WT *H pylori* at different MOI (24 hours) or at the indicated time points (MOI = 100). For signal pathway inhibition experiments, AGS cells were pretreated with 5 μL (20 μM) U0126 (an MEK-1 and MEK-2 inhibitor), SB203580 (a p38 MAPK inhibitor), SP600125 (a JNK inhibitor), FLLL32 (an STAT3 inhibitor), AG490 (a JAK inhibitor), Wortmannin (a PI3K-AKT inhibitor), PP2 (a *cagA* EPIYA motif phosphorylation inhibitor), or DMSO control for 2 hours. For Rev-erbα activation or inhibition experiments, AGS cells were pretreated with *Rev-erbα* siRNA, NC (40 nM), or lipofectamine 2000 only (Mock) for 24 hours. In some cases, AGS cells were transfected with plasmids pcDNA3.1 or *cagA*-pcDNA3.1 by using lipofectamine 2000 according to the manufacturer's protocols. At 24 hours after transfection, cells were treated with or without U0126 (5 μL, 20 μM) or DMSO control for 2 hours and cultured for an additional 24 hours. After co-culture, cells were collected for immunofluorescence, real-time PCR, and Western blot, and the culture supernatants were harvested for ELISA.

In Vitro Bactericidal Assay

Two hundred microliters of 5×10^6 CFU/mL WT *H pylori* suspension was incubated with 20 μg/mL mouse Reg3b or β-defensin-1 for 3, 6, or 12 hours, or incubated with 5, 10, or 20 μg/mL mouse Reg3b or β-defensin-1 for 24 hours. PBS was used as control. In another set of experiments, primary GECs from WT or *Rev-erbα*$^{-/-}$ mice were infected with WT *H pylori* (MOI = 100) for 24 hours. The culture supernatants were filtered through 0.4-μm filters and collected. Then 200 μL of 5×10^6 CFU/mL WT *H pylori* suspension were incubated with the above collected culture supernatants with or without anti-Reg3b or anti-β-defensin-1 Abs (20 μg/mL) for 24 hours. Bacteria were serially diluted and plated on brain-heart infusion plates containing 10% rabbit blood and incubated for 3–5 days at 37°C under microaerophilic conditions and CFU was enumerated. The results was determined by counting CFU of alive bacteria with agar plating and expressed as the survival rate of WT *H pylori* after incubation with Reg3b/β-defensin-1 or PBS, or was determined by counting CFU of alive bacteria with agar plating and expressed as the survival rate of WT *H pylori* after incubation with supernatants from *H pylori*–infected GECs of *Rev-erbα*$^{-/-}$ mice or WT mice with or without anti-Reg3b or anti-β-defensin-1 Abs.

In Vitro T Cell Culture System

Purified mouse peripheral or spleen $CD4^+$ T cells from uninfected or WT *H pylori*–infected WT mice (8 week p.i.) were labeled with carboxyfluorescein succinimidyl ester and co-cultured (1×10^5 cells/well) with fluorescence-activated cell sorter (FACS)–sorted gastric $CD45^+CD11c^-Ly6G^-CD11b^+CD68^-$ myeloid cells from WT *H pylori*–infected WT mice (8 week p.i.) at 2:1 ratio in 200 μL RPMI 1640 medium containing mouse recombinant IL-2 (20 IU/mL), anti-CD3 (2 μg/mL), and anti-CD28 (1 μg/mL) Abs. After a 5-day incubation, cells were collected and analyzed by intracellular cytokine staining, and the culture supernatants were harvested for ELISA.

Chemotaxis Assay

Human $CD45^+CD11c^-CD66b^-CD11b^+CD68^-$ myeloid cells or mouse $CD45^+CD11c^-Ly6G^-CD11b^+CD68^-$ myeloid cells from blood of *H pylori*–infected donors or WT *H pylori*–infected mice (8 week p.i.) were sorted by FACS (FACSAria II; BD Biosciences, Franklin Lakes, NJ). AGS cells were pretreated with *Rev-erbα* siRNA or NC (both at 40 nM) for 24 hours, and then infected with WT *H pylori* or *ΔcagA* (MOI = 100) for 24 hours. The culture supernatants were filtered through 0.4-μm filters, collected and used as source of chemoattractants in a human myeloid cell chemotaxis assay. In another set of experiments, mouse primary GECs were purified from gastric tissue single-cell suspensions of uninfected WT or *Rev-erbα*$^{-/-}$ mice with anti-mouse CD326-conjugated MACS magnetic beads, and then infected with WT *H pylori* or *ΔcagA* (MOI = 100) for 24 hours. The culture supernatants were then collected mentioned above. These culture supernatants were then used as source of chemoattractants in a mouse myeloid cell chemotaxis assay.

In a chemotaxis assay, FACS-sorted myeloid cells (1×10^5) were transferred into the upper chambers of the transwells (5-μm pore). CCL21 (100 ng/mL) and culture supernatants from various cultures were placed in the lower chambers. After 6 hours culture, migration was quantified by counting cells in the lower chamber and cells adhering to the bottom of the membrane. In some cases, blocking Ab for human/mouse CCL21 (20 μg/mL) or corresponding control IgG/IgG2a (20 μg/mL) were added into the culture supernatants, and blocking Ab for human/mouse CCR7 (20 μg/mL) or corresponding control IgG2a (20 μg/

Table 2. Antibodies and Other Reagents

Antibodies and Reagents	Manufacturer
Antibodies for flow cytometry	
anti-mouse CD45-PE-Cy7(103114)	BioLegend
anti-mouse Ly6G-FITC (127605)	BioLegend
anti-mouse CD11c-PerCP-Cy5.5(117327)	BioLegend
anti-mouse CD3-APC (300311)	BioLegend
anti-mouse NK1.1-PE (108707)	BioLegend
anti-mouse CD19-APC-Cy7(115529)	BioLegend
anti-mouse CD11b-PE (101207)	BioLegend
anti-mouse CD68-APC-Cy7(137023)	BioLegend
anti-mouse CCR7-APC (120108)	BioLegend
anti-mouse Ly6C-APC (128016)	BioLegend
anti-mouse F4/80-APC (123116)	BioLegend
anti-human CD45-PE-Cy7(368532)	BioLegend
anti-human CD66b-FITC (305104)	BioLegend
anti-human CD11c-PerCP-Cy5.5(301624)	BioLegend
anti-human CD11b-PE (301306)	BioLegend
anti-human CD68-APC-Cy7(333822)	BioLegend
anti-human CCR7-APC (353214)	BioLegend
anti-mouse CD4-PerCP-Cy5.5(100433)	BioLegend
anti-mouse IFN-γ-APC (505810)	BioLegend
anti-mouse CCR7-Brilliant Violet 605 (120125)	BioLegend
anti-mouse CD163-Brilliant Violet 421 (155309)	BioLegend
anti-mouse CD206-Alexa Fluor 647 (141711)	BioLegend
anti-mouse MHC II Brilliant Violet 510 (107635)	BioLegend
anti-mouse IL-12-APC (505205)	BioLegend
anti-mouse IL-10-Brilliant Violet 421 (505021)	BioLegend
Antibodies for immunohistochemical staining	
rabbit anti-human/mouse Rev-erbα(ab174309, 1:100)	Abcam
horseradish peroxidase anti-rabbit IgG (ZB-2301)	Zhongshan Biotechnology
sheep anti-mouse Reg3b (AF5110)	R&D Systems
horseradish peroxidase anti-sheep IgG (ZB-2306)	Zhongshan Biotechnology
rabbit anti-mouse β-defensin-1(PA5-75666)	Thermo Fisher Scientific
Antibodies for immunofluorescence	
rabbit anti-human/mouse Rev-erbα(ab174309;ab251057, 1:100)	Abcam
mouse anti-human/mouse CD326 (EpCAM) (ab212580, 1:100)	Abcam
rabbit anti-human CCL21(ab231116;ab248260, 1:100)	Abcam
rabbit anti-human/mouse pepsinogen II (ab259997, 1:100)	Abcam
rabbit anti-mouse CD11b (ab232427, 1:100)	Abcam
rat anti-mouse Ly6C (ab15627, 1:100)	Abcam
mouse anti-*H pylori* (188-10881-1, 1:100)	RayBiotech
goat anti-rabbit-TRITC (ZF-0316, 1:50)	Zhongshan Biotechnology
goat anti-rabbit-FITC (ZF-0311, 1:50)	Zhongshan Biotechnology
goat anti-mouse-TRITC (ZF-0313, 1:50)	Zhongshan Biotechnology
goat anti-mouse-FITC (ZF-0312, 1:50)	Zhongshan Biotechnology
goat anti-rat-FITC (ZF-0315, 1:50)	Zhongshan Biotechnology
Antibodies for neutralizing and blocking	
anti-human CCL21 (Goat IgG) (AF366)	R&D Systems
Goat IgG Control (AB-108-C)	R&D Systems
anti-human CCR7 (Mouse IgG2a) (MAB197)	R&D Systems
Mouse IgG2a Isotype Control (MAB003)	R&D Systems
anti-mouse CCL21 (Rat IgG2a) (MAB457)	R&D Systems
anti-mouse CCR7 (Rat IgG2a) (MAB3477)	R&D Systems
Rat IgG2a Isotype Control (MAB006)	R&D Systems
anti-mouse Reg3b (MAB5110)	R&D Systems
anti-mouse β-defensin-1(PA5-75666)	Thermo Fisher Scientific
Antibodies for Western blot	
rabbit anti-human/mouse Rev-erbα(ab174309, 1:1000)	Abcam
rabbit anti-human ERK1/2(4695, 1:1000)	Cell Signaling Technology
rabbit anti-human ERK1/2(ab218017, 1:1000)	Abcam
rabbit anti-human p-ERK1/2(4370S, 1:2000)	Cell Signaling Technology
rabbit anti-human p-ERK1/2(ab242418, 1:2000)	Abcam
rabbit anti-human/mouse GAPDH (BL042F, 1:1000)	Beijing Ray Antibody Biotech
rabbit anti-human/mouse GAPDH (ab186930;ab199554, 1:1000)	Abcam
rabbit anti-human/mouse Lamin B1(ab133741;ab220797, 1:1000)	Abcam
rabbit anti-*cagA*(sc-28368, 1:100)	Santa Cruz Biotechnology

Table 2. Continued

Antibodies and Reagents	Manufacturer
ELISA kits	
mouse Reg3b (ml058487-C)	ML Bio
mouse β-defensin-1(ml002270-C)	ML Bio
human CCL21(ELH-6Ckine-1)	RayBiotech
mouse CCL21(ELM-6Ckine)	RayBiotech
mouse IFN-γ(1210002)	Dakewe Biotech Co
Reagents for signaling pathways inhibition	
MEK-1 and MEK-2 inhibitor U0126(U120)	Merk Millipore
MAPK inhibitor SB203580(S8307)	Calbiochem
JNK inhibitor SP600125(S5567)	Calbiochem
STAT3 phosphorylation inhibitor FLLL32(406111)	MedKoo Biosciences
JAK inhibitor AG490(200121)	Merk Millipore
PI3K-AKT inhibitor Wortmannin (406447)	Merk Millipore
Reagents for Luciferase Reporter Assay	
Dual-luciferase reporter assay system (E1910)	Promega
Endo-free Plasmid Mini Kit (D6950)	Omega
Pierce Magnetic CHIP Kit (26157)	Thermo Fisher Scientific
truChIP Chromatin Shearing Kit (520127)	Covaris
16% Formaldehyde, Methanol-Free (12606)	Cell Signaling Technology
Antibodies for CHIP	
Rev-erbα rabbit mAb (13418s, 1:100)	Cell Signaling Technology
NF-κB p65 rabbit mAb (8242s, 1:100)	Cell Signaling Technology
SimpleChip human NR1D1 promoter primers (13413s)	Cell Signaling Technology
Purified anti-CD3 antibodies (100201)	BioLegend
Purified anti-CD28 antibodies (102101)	BioLegend
Human CD326 microbeads (130-061-101)	Miltenyi Biotec
Mouse CD326 microbeads (130-105-958)	Miltenyi Biotec
EasySep Mouse CD4+ T Cell Isolation Kit (19852)	StemCell Technologies
Dynabeads FlowComp Mouse CD4 Kit	Invitrogen
5-μm pore size Transwells (3421)	Corning
0.4-μm pore size Transwells (3413)	Corning
Collagenase IV (17104019)	Gibco
DNase I (AMPD1)	Sigma-Aldrich
Phorbol myristate acetate (P8139)	Sigma-Aldrich
Ionomycin (407951)	Sigma-Aldrich
Golgistop (554724)	BD Pharmingen
Perm/Wash solution (554714)	BD Pharmingen
Carboxylfluorescein succinimidyl ester (CFSE) (65-0850-84)	eBioscience
Rev-erbα agonist SR9009(554726)	Merck
Rev-erbα antagonist SR8278(554718)	Merck
Cremophor (61791-12-6)	BASF
DMSO (D2650)	Sigma-Aldrich
Protein Extraction Reagent (89901)	Pierce
SuperSignal West Dura Extended Duration Substrate kit (34075)	Thermo
Fetal bovine serum (FBS) (10091148)	Gibco
Fetal bovine serum (FBS) (10099141C)	Invitrogen
Penicillin/Streptomycin (15140122)	Gibco
RPMI-1640(SH30809.01)	Hyclone
DMEM/F12 (1:1) (SH30023.01)	Hyclone
Ficoll-Paque Plus (17-1440-02)	GE Healthcare
lyses solution (RT122)	TIANGEN
TRIzol reagent (15596026)	Invitrogen
Lipofectamine 2000 Transfection Reagent (11668027)	Invitrogen
Lipofectamine RNAiMAX Transfection Reagent (13778150)	Invitrogen
QIAamp DNA Mini Kit (51304)	QIAGEN

Table 2. Continued

Antibodies and Reagents	Manufacturer
PrimeScript RT reagent Kit (R037A)	TaKaRa
Real-time PCR Master Mix (QPK-201)	Toyobo
pGL3-basic vector (E1751)	Promega
Recombinant mouse Reg3b (5110-RG)	R&D Systems
Recombinant mouse β-defensin-1(228-11913-1)	RayBiotech
Recombinant mouse CCL21(457-6C)	R&D Systems
Recombinant human CCL21(366-6C)	R&D Systems
All other recombinant human/mouse cytokines and chemokines	PeproTech

APC, allophycocyanin; APC-Cy7, allophycocyanin-cyanin 7; ChIP, chromatin immunoprecipitation; FITC, fluorescein isothiocyanate; IFN, interferon; PE, phycoerythrin; PE-Cy7, phycoerythrin-cyanin 7; PerCP-Cy5.5, peridin chlorophyl protein-cyanin 5.5.

mL) were added into myeloid cell suspensions and incubated for 2 hours before chemotaxis assays.

Immunohistochemistry

Paraformaldehyde-fixed and paraffin-embedded samples were cut into 5-μm sections. For immunohistochemical staining, the sections were incubated with rabbit anti-human/mouse Rev-erbα, sheep anti-mouse Reg3b, or rabbit anti-mouse β-defensin-1 followed by horseradish peroxidase (HRP)–conjugated anti-rabbit IgG or HRP-conjugated anti-sheep IgG and later its substrate diaminobenzidine. All the sections were finally counterstained with hematoxylin and examined using a microscope (Nikon Eclipse 80i; Nikon, Tokyo, Japan).

Immunofluorescence

Paraformaldehyde-fixed cryostat tissue sections or AGS cells were washed in PBS, blocked for 30 minutes with 20% goat serum in PBS, stained for Rev-erbα, Rev-erbα and CD326, CCL21 and CD326, Rev-erbα and pepsinogen II, Ly6C and CD11b, or Rev-erbα and *H pylori*. Slides were examined with a confocal fluorescence microscope (LSM 510 META, Zeiss, Oberkochen, Germany).

Real-Time PCR

DNA of the biopsy specimens were extracted with QIAamp DNA Mini Kit and RNA of biopsy specimens and cultured cells were extracted with TRIzol reagent (Thermo Fisher Scientific, Waltham, MA). The RNA samples were reversed transcribed into complementary DNA with PrimeScript RT reagent Kit (Takara Bio, Mountain View, CA). Real-time PCR was performed on an IQ5 (Bio-Rad, Hercules, CA) with Real-time PCR Master Mix according to the manufacturer's specifications. The mRNA expression of 16s rDNA, *cagA*, Rev-erbα, chemokine, IFN-γ, β-defensin and Reg3 genes was measured using the TaqMan or SYBR green method with the relevant primers (Table 3). For mouse samples, mouse β2-microglobulin mRNA level served as a normalizer, and its level in the stomach of uninfected or WT mice served as a calibrator. For human samples, human β-actin mRNA level served as a normalizer, and its level in the uninfected cells/tissues or stomach of uninfected donors served as a calibrator. The relative gene expression was expressed as fold change of relevant mRNA calculated by the ΔΔCt method.

Luciferase Reporter Assay

Promoter constructs containing the region from −2000 to 0, −1000 to 0, −500 to 0, −250 to 0, −100 to 0, and other 250-bp fragments of *Rev-erbα* gene were amplified from human genomic DNA using specifically designed primers (Table 4) by PCR. The amplified full-length or fragmented sequences were cloned into the NheI and HindIII sites of the pGL3-basic vector respectively. Promoter constructs containing the region from -2000 to 0 of *CCL21* and *β-defensin-1* gene, and mutants of predicted Rev-erbα binding site of *CCL21* and *β-defensin-1* gene sequences were also synthesized with primers (Table 5) and cloned into the NheI and HindIII sites of the pGL3-basic vector respectively. The above constructs were sequence verified. Plasmids overexpressing Rev-erbα (*Rev-erbα*-pcDNA3.1) were constructed by inserting target gene into plasmid pcDNA3.1, these plasmids were constructed and produced by Sangon Biotech (Shanghai, China). Cells were transfected with various combinations of the reporter plasmid, which contains the internal control pRL-TK (Promega, Madison, WI) or the expression plasmid. Cells were harvested at 24 hours (*H pylori* infection assay) or 48 hours (*cagA*-pcDNA3.1 or *Rev-erbα*-pcDNA3.1 plasmid transfection assay) after transfection. Luciferase activities of the lysates were measured using the Dual-Luciferase Reporter Assay Kit (Promega) following the manufacturer's protocol. Luciferase activity was normalized to *Renilla* luciferase activity.

Chromatin Immunoprecipitation

AGS cells infected with *H pylori* (MOI = 100, 24 hours) were treated at room temperature for 10 minutes with 1% formaldehyde in cell culture media. Glycine (11% in media) solution was then gently mixed in at room temperature for 5 minutes to terminate cross-linking. Cells were washed twice with ice-cold PBS and palleted at 3000 g for 5 minutes. Membrane Extraction Buffer containing protease/phosphatase inhibitors was then added to each palleted sample. Cell lysates were pulse-sonicated on ice;

Table 3. Primer and Probe Sequences for Real-Time PCR Analysis

Gene	Primer or Probe	Sequence 5′→3′
H pylori 16s rDNA	forward	TTTGTTAGAGAAGATAATGACGGTATCTAAC
	reverse	CATAGGATTTCACACCTGACTGACTATC
	probe	CGTGCCAGCAGCCGCGGT
Mouse *β2-microglobulin*	forward	CCTGCAGAGTTAAGCATGCCAG
	reverse	TGCTTGATCACATGTCTCGATCC
	probe	TGGCCGAGCCCAAGACCGTCTAC
H pylori cagA	forward	GAGTCATAATGGCATAGAACCTGAA
	reverse	TTGTGCAAGAAATTCCATGAAA
Mouse *Sry*	forward	TGGGACTGGTGACAATTGTC
	reverse	GAGTACAGGTGTGCAGCTCT
Human *Rev-erbα*	forward	TCAGCTGGTGAAGACATGACGAC
	reverse	GGAGCCACTGGAGCCAATGTA
Human *GAPDH*	forward	ACCCAGAAGACTGTGGATGG
	reverse	CAGTGAGCTTCCCGTTCAG
Human *CCL21*	forward	TATCCTGGTTCTGGCCTTTG
	reverse	CAGCCTAAGCTTGGTTCCTG
Human *β-defensin-1*	forward	CCAGTCGCCATGAGAACTTCC
	reverse	GTGAGAAAGTTACCACCTGAGGC
Mouse *Rev-erbα*	forward	GCTTCTCTCAGTTCCCACAAC
	reverse	GGTGAAGATTTCTCGATGGGC
Mouse *β-actin*	forward	AGTGTGACGTTGACATCCGT
	reverse	GCAGCTCAGTAACAGTCCGC
Mouse *CCL1*	forward	ATGGCACTGATGTGCCTGCT
	reverse	GGTGGAGGACTGAGGGAAA
Mouse *CCL2*	forward	TCACCTGCTGCTACTCATTCA
	reverse	CACTGTCACACTGGTCACTCC
Mouse *CCL3*	forward	TTCTCTGTACCATGACACTCTGC
	reverse	CGTGGAATCTTCCGGCTGTAG
Mouse *CCL4*	forward	TGTCTGCCCTCTCTCTCCTCT
	reverse	AGCAAGGACGCTTCTCAGTGA
Mouse *CCL5*	forward	GCTGCTTTGCCTACCTCTCC
	reverse	TCGAGTGACAAACACGACTGC
Mouse *CCL6*	forward	CCAAGACTGCCATTTCATTC
	reverse	AAGCAATGACCTTGTTCCCA
Mouse *CCL7*	forward	ATGGAAGTCTGCGCTGAAG
	reverse	ACATGAGGTCTCCAGAGCTTT
Mouse *CCL8*	forward	ACGCTAGCCTTCACTCCAAAA
	reverse	TTCCAGCTTTGGCTGTCTCTT
Mouse *CCL9*	forward	TGGCATATCTGGCTTTGTCA
	reverse	ATGGCTGTAGCTCAAGATGGT
Mouse *CCL11*	forward	TCCACAGCGCTTCTATTCCT
	reverse	GCAGTTCTTAGGCTCTGGGTT
Mouse *CCL12*	forward	TCGAAGTCTTTGACCTCAACA
	reverse	GGGAACTTCAGGGGGAAATA
Mouse *CCL19*	forward	ACTTGCACTTGGCTCCTGAA
	reverse	AGTCTTCCGCATCATTAGCA
Mouse *CCL20*	forward	GCAAGCGTCTGCTCTTCCTT
	reverse	TTAGGCTGAGGAGGTTCACA
Mouse *CCL21*	forward	GATGATGACTCTGAGCCTCCT
	reverse	TTCTGCACCCAGCCTTCCT

Table 3. Continued

Gene	Primer or Probe	Sequence 5′→3′
Mouse *CCL22*	forward	TGGCAATTCAGACCTCTGATG
	reverse	TTGCTGGAATGGCAGAAGAA
Mouse *CCL24*	forward	TCATCTTGCTGCACGTCCTTT
	reverse	TAAACCTCGGTGCTATTGCCA
Mouse *CCL25*	forward	TCTCAGGACCAGAAAGGCATT
	reverse	TGGCGGAAGTAGAATCTCACA
Mouse *CCL27*	forward	AGGCTGAGTGAGCATGATGGA
	reverse	TTGGCGTTCTAACCACCGA
Mouse *CCL28*	forward	GCTGTGTGTGTGGCTTTTCAA
	reverse	TACCTCTGAGGCTCTCATCCA
Mouse *CX3CL1*	forward	TGGCTTTGCTCATCCGCTATCAG
	reverse	CGTCTGTGCTGTGTCGTCTCC
Mouse *CXCL1*	forward	ACCCAAACCGAAGTCATAG
	reverse	TTGTATAGTGTTGTCAGAAGC
Mouse *CXCL2*	forward	ACTTCAAGAACATCCAGAG
	reverse	CTTTCCAGGTCAGTTAGC
Mouse *CXCL3*	forward	CAGCCACACTCCAGCCTA
	reverse	CACAACAGCCCCTGTAGC
Mouse *CXCL4*	forward	AGCGATGGAGATCTTAGCTGTGT
	reverse	CCAGGCTGGTGATGTGCTTAA
Mouse *CXCL5*	forward	AGTCAAGAATCATTGGTTGTTAACCTT
	reverse	TCCGGAGACAATGCAATAGTCA
Mouse *CXCL7*	forward	GGAGTTCACTGTGCTGATGTGGA
	reverse	CACAGATGAAGCAGCTGGTCAGTAA
Mouse *CXCL9*	forward	ACAAATCCCTCAAAGACCTCAAACAG
	reverse	ATCTCCGTTCTTCAGTGTAGCAATG
Mouse *CXCL10*	forward	TGAAAGCGTTTAGCCAAAAAAGG
	reverse	AGGGGAGTGATGGAGAGAGG
Mouse *CXCL12*	forward	CCTCCAAACGCATGCTTCA
	reverse	ACTCTCCTCCCTTCCATTGCA
Mouse *CXCL13*	forward	CAGGCCACGGTATTCTGGA
	reverse	CAGGGGGCGTAACTTGAATC
Mouse *CXCL14*	forward	GCTTCATCAAGTGGTACAAT
	reverse	CTGGCCTGGAGTTTTTCTTTCCAT
Mouse *CXCL15*	forward	CTAGGCATCTTCGTCCGTCC
	reverse	TTGGGCCAACAGTAGCCTTC
Mouse *CXCL16*	forward	AAACATTTGCCTCAAGCCAGT
	reverse	GTTTCTCATTTGCCTCAGCCT
Mouse *CXCL17*	forward	ATGAAGCTTCTAGCCTCTCCC
	reverse	CTATAAGGGCAGCGCAAAGCTTGC
Mouse *β-defensin-1*	forward	GAACACGGTACACAGGCTTCC
	reverse	CCTGAATCACAGATGTCCAAG
Mouse *β-defensin-2*	forward	CTCTCTGGAGTCTGAGTGCCC
	reverse	AGGACGCCTGGCAGAAGGAGG
Mouse *β-defensin-3*	forward	TGCTGCTGTCTCCACCTGC
	reverse	AGTGTTGCCAATGCACCGAT
Mouse *β-defensin-4*	forward	ACATGCATGACCAATGGAGCC
	reverse	CATCTTGCTGGTTCTTC
Mouse *Reg3a*	forward	CTGCTCTCCTGCCTGTTGTT
	reverse	GGAGCGATAAGCCTTGTAACC

Table 3. Continued

Gene	Primer or Probe	Sequence 5′→3′
Mouse *Reg3b*	forward	AGGCTTATGGCTCCTACTGCT
	reverse	GAAGCCTCAGCGCTATTGAG
Mouse *Reg3g*	forward	TGCCTATGGCTCCTATTGCT
	reverse	CATGGAGGACAGGAAGGAAG
Mouse *Reg3d*	forward	CTGTCTTCTCCACGCATCAG
	reverse	CTGCTCCACTTCCATCCATT

NOTE. For the probes, a FAM fluorescent reporter is coupled to the 5' end, and a TAMRA quencher is coupled to the 3' end.

supernatants containing the digested chromatin were collected into two tubes for input and immunoprecipitation. Anti-NF-κB p65 or anti-Rev-erbα Ab was added and IP reactions conducted overnight at 4°C with agitation. ChIP grade protein A/G magnetic beads were then added to each IP reaction. Two hours later beads were collected, washed, bounded IP materials eluted with 5 M NaCl containing 20 μg/mL Proteinase K. The cross-linking was reversed by heating up to 65°C for 1.5 hours and DNA was purified. Purified DNA samples were analyzed by PCR with designed primers (Table 6).

Flow Cytometry

Cell surface markers were stained with specific or isotype control Abs. For intracellular molecules measurements, the cells were stimulated for 5 hours with phorbol myristate acetate (50 ng/mL) plus ionomycin (1 μg/mL) in the presence of Golgistop (BD Biosciences). Intracellular cytokine staining was performed after fixation and permeabilization, using Perm/Wash solution. Then, the cells were analyzed by multicolor flow cytometry on FACSCanto II and FACSCanto (BD Biosciences). Data were analyzed with FlowJo software (TreeStar, Ashland, OR) or FACSDiva software (BD Biosciences).

Enzyme-Linked Immunosorbent Assay

Isolated human and mouse gastric tissues were homogenized in 1 mL sterile Protein Extraction Reagent, and centrifuged. Tissue supernatants were collected for ELISA. Concentrations of CCL21, Reg3b, β-defensin-1, or IFN-γ in

Table 4. Primers for Amplify Full-Length and the Different Fragment Sequences of *Rev-erb*α Gene for PCR

Name	Primer	Sequence 5′→3′
Human *Rev-erb*α (–2000/0)	forward	GCTCTTACGCGTGCTAGCTGCCTGTGGAGAAGGGCTTC
	reverse	TACCGGAATGCCAAGCTTGTCTTCACCAGCTGAGAGCG
Human *Rev-erb*α (–1000/0)	forward	GCTCTTACGCGTGCTAGCCCCGGTCACCAGTAACCTC
	reverse	CAGTACCGGAATGCCAAGC
Human *Rev-erb*α (–500/0)	forward	GCTCTTACGCGTGCTAGCTTGGCAGAGTGAAATATTACTGC
	reverse	CAGTACCGGAATGCCAAGC
Human *Rev-erb*α (–250/0)	forward	GCTCTTACGCGTGCTAGCTGATTCCCCCTACACACTCTC
	reverse	CAGTACCGGAATGCCAAGC
Human *Rev-erb*α (–100/0)	forward	GCTCTTACGCGTGCTAGCTCCCCGCCCTTAGCCAGT
	reverse	CAGTACCGGAATGCCAAGC
Human *Rev-erb*α (–2000/–1750)	forward	GCTCTTACGCGTGCTAGCATCAATACCATCCCAGGAGCTGCCTGTGGAGAAGGG
	reverse	TACCGGAATGCCAAGCTTAAAACAGCCAGTATTTCGCTTC
Human *Rev-erb*α (–1749/–1500)	forward	GCTCTTACGCGTGCTAGCTTGTTTGTTTGTTTTGGAGACAG
	reverse	TACCGGAATGCCAAGCTTCTGAGGTGGGTTGATCACCTG
Human *Rev-erb*α (–1499/–1250)	forward	GCTCTTACGCGTGCTAGCCCTCACAAAGTGCTGGGATT
	reverse	TACCGGAATGCCAAGCTTAATTCCACAGAAGATTACTACTCAG
Human *Rev-erb*α (–1249/–1000)	forward	GCTCTTACGCGTGCTAGCCATATTTTATCCTCCAGCACCG
	reverse	TACCGGAATGCCAAGCTTTCCAGGGGAAGGAGTTCC
Human *Rev-erb*α (–999/–750)	forward	GCTCTTACGCGTGCTAGCGGTGTTCTCCCTAAGGCGAG
	reverse	TACCGGAATGCCAAGCTTGCAAGCTTGTTTGCTGTCTG
Human *Rev-erb*α (–749/–500)	forward	GCTCTTACGCGTGCTAGCCAGTCCCTCCCCAGAAATTC
	reverse	TACCGGAATGCCAAGCTTCAGTGACACACTTTTCCAACAGC

Table 5. Primers for Amplify Full-Length Sequences of *CCL21* and *β-Defensin-1* Gene for PCR and Sequences of Heterologous Reporter Constructs

Name	Sequence 5′→3′
CCL21 promoter	GCTCTTACGCGTGCTAGCAAAGACTGAAGAAAAAAAAAAGTCAAAC
	TACCGGAATGCCAAGCTTTTGGGGGTCTGTGCGTGG
Original sequence	682 ttg agg tca ggc 694
CCL21 promoter mutant	GCTCTTACGCGTGCTAGCAAAGACTGAAGAAAAAAAAAAGTCAAAC
	CCGTCTAGAGGAGCAGTGAGATTGTGGAAAG
	ATCTCACTGCTCCTCTAGACGGCATGGCTCAGCCTCTTC
	CCGTCTAGAGGAGCAGTGAGATTGTGGAAAG
Mutant sequence	682 ttg cta gac ggc 694
β-defensin-1 promoter	GCTCTTACGCGTGCTAGCGGTGGGATTACAGGTGTGTGC
	TACCGGAATGCCAAGCTTGGTGAACTTCTAATCGCTAACCCC
Original sequence	754 cct agg tca ggc 766
β-defensin-1 promoter mutant	GCTCTTACGCGTGCTAGCAAAGACTGAAGAAAAAAAAAAGTCAAAC
	CCGTCTAGAGGAGCAGTGAGATTGTGGAAAG
	ATCTCACTGCTCCTCTAGACGGCATGGCTCAGCCTCTTC
	CCGTCTAGAGGAGCAGTGAGATTGTGGAAAG
Mutant sequence	754 cct cta gac ggc 766

PCR, polymerase chain reaction.

the tissue supernatants; concentrations of CCL21, Reg3b, or β-defensin-1 in the gastric epithelial cell culture supernatants; and concentrations of IFN-γ in the T cell culture supernatants were determined using ELISA kits according to the manufacturer's instructions.

Western Blot Analysis

Western blots were performed on 10%–15% sodium dodecyl sulfate polyacrylamide gel electrophoresis gel transferred polyvinylidene difluoride membranes with equivalent amounts of cell or tissue lysate protein for each sample. Five percent skim milk was used for blocking the polyvinylidene difluoride membranes. Mouse Rev-erbα, ERK1/2, and p-ERK1/2 were detected with rabbit anti-Rev-erbα Ab, rabbit anti-ERK1/2 Ab, and rabbit anti-p-ERK1/2 Ab; human Rev-erbα, ERK1/2, and p-ERK1/2 were detected with rabbit anti-Rev-erbα Ab, rabbit anti-ERK1/2 Ab, and rabbit anti-p-ERK1/2 Ab; *cagA* was detected with rabbit anti-*cagA* Ab respectively. This was followed by incubation with HRP-conjugated secondary Abs. Bound proteins were visualized by using SuperSignal West Dura Extended Duration Substrate kit (Thermo Fisher Scientific).

Table 6. Primers for ChIP PCR analysis

Gene	Primer	Sequence 5′→3′
β-defensin-1	forward	AGCAAGGAAAGCTGTGTTTCGG
	reverse	GATGCAGTGGGATCCTGTAGCT
CCL21	forward	GGAGCGTAGTGAGGAGACAGT
	reverse	GGGCCTGAGCCTTCCTTCTAT

NOTE. Primers for ChIP analysis of *β-defensin-1* and *CCL21* were designed and produced by Sangon Biotech (Shanghai, China). Primers for *Rev-erbα* purchased in Cell Signaling Technology pathway (Cat#:13413).
ChIP, chromatin immunoprecipitation; PCR, polymerase chain reaction.

Statistical Analysis

Results are expressed as mean ± SEM. Student's *t* test was generally used to analyze the differences between two groups, but when the variances differed, the Mann-Whitney *U* test was used. For multiple comparisons, the 1-way analysis of variance was used. Correlations between parameters were assessed using Pearson correlation analysis and linear regression analysis, as appropriate. SPSS statistical software (version 13.0; SPSS Inc, Chicago, IL) was used for all statistical analysis. All data were analyzed using 2-tailed tests, and $P < .05$ was considered statistically significant. Microarray data analysis was performed with the assistance of Genminix Informatics (Shanghai, China). Raw data from each array were analyzed using TwoClassDif.

References

1. Hooi JKY, Lai WY, Ng WK, Suen MMY, Underwood FE, Tanyingoh D, Malfertheiner P, Graham DY, Wong VWS, Wu JCY, Chan FKL, Sung JJY, Kaplan GG, Ng SC. Global prevalence of Helicobacter pylori infection: systematic review and meta-analysis. Gastroenterology 2017;153:420–429.

2. Jin HS, Kim TS, Jo EK. Emerging roles of orphan nuclear receptors in regulation of innate immunity. Arch Pharm Res 2016;39:1491–1502.
3. Mazaira GI, Zgajnar NR, Lotufo CM, Daneri-Becerra C, Sivils JC, Soto OB, Cox MB, Galigniana MD. The nuclear receptor field: a historical overview and future challenges. Nucl Receptor Res 2018;5:101320.
4. Pourcet B, Zecchin M, Ferri L, Beauchamp J, Sitaula S, Billon C, Delhaye S, Vanhoutte J, Mayeuf-Louchart A, Thorel Q, Haas JT, Eeckhoute J, Dombrowicz D, Duhem C, Boulinguiez A, Lancel S, Sebti Y, Burris TP, Staels B, Duez HM. Nuclear receptor subfamily 1 group D member 1 regulates circadian activity of NLRP3 inflammasome to reduce the severity of fulminant hepatitis in mice. Gastroenterology 2018;154:1449–1464.e20.
5. Kojetin DJ, Burris TP. REV-ERB and ROR nuclear receptors as drug targets. Nat Rev Drug Discov 2014;13:197–216.
6. Curtis AM, Bellet MM, Sassone-Corsi P, O'Neill LA. Circadian clock proteins and immunity. Immunity 2014;40:178–186.
7. Feng D, Liu T, Sun Z, Bugge A, Mullican SE, Alenghat T, Liu XS, Lazar MA. A circadian rhythm orchestrated by histone deacetylase 3 controls hepatic lipid metabolism. Science 2011;331:1315–1319.
8. Duez H, van der Veen JN, Duhem C, Pourcet B, Touvier T, Fontaine C, Derudas B, Baugé E, Havinga R, Bloks VW, Wolters H, van der Sluijs FH, Vennström B, Kuipers F, Staels B. Regulation of bile acid synthesis by the nuclear receptor Rev-erbalpha. Gastroenterology 2008;135:689–698.
9. Cho H, Zhao X, Hatori M, Yu RT, Barish GD, Lam MT, Chong LW, DiTacchio L, Atkins AR, Glass CK, Liddle C, Auwerx J, Downes M, Panda S, Evans RM. Regulation of circadian behaviour and metabolism by REV-ERB-alpha and REV-ERB-beta. Nature 2012;485:123–127.
10. Pariollaud M, Gibbs JE, Hopwood TW, Brown S, Begley N, Vonslow R, Poolman T, Guo B, Saer B, Jones DH, Tellam JP, Bresciani S, Tomkinson NC, Wojno-Picon J, Cooper AW, Daniels DA, Trump RP, Grant D, Zuercher W, Willson TM, MacDonald AS, Bolognese B, Podolin PL, Sanchez Y, Loudon AS, Ray DW. Circadian clock component REV-ERBalpha controls homeostatic regulation of pulmonary inflammation. J Clin Invest 2018;128:2281–2296.
11. Chandra V, Bhagyaraj E, Nanduri R, Ahuja N, Gupta P. NR1D1 ameliorates Mycobacterium tuberculosis clearance through regulation of autophagy. Autophagy 2015;11:1987–1997.
12. Chandra V, Bhagyaraj E, Nanduri R, Ahuja N, Gupta P. Human IL10 gene repression by Rev-erbalpha ameliorates Mycobacterium tuberculosis clearance. J Biol Chem 2013;288:10692–10702.
13. Gagnidze K, Hajdarovic KH, Moskalenko M, Karatsoreos IN, McEwen BS, Bulloch K. Nuclear receptor REV-ERBalpha mediates circadian sensitivity to mortality in murine vesicular stomatitis virus–induced encephalitis. Proc Natl Acad Sci U S A 2016;113:5730–5735.
14. Amieva M, Peek RM Jr. Pathobiology of Helicobacter pylori-induced gastric cancer. Gastroenterology 2016;150:64–78.
15. Suzuki M, Mimuro H, Kiga K, Fukumatsu M, Ishijima N, Morikawa H, Nagai S, Koyasu S, Gilman RH, Kersulyte D, Berg DE, Sasakawa C. Helicobacter pylori CagA phosphorylation-independent function in epithelial proliferation and inflammation. Cell Host Microbe 2009;5:23–34.
16. Mueller D, Tegtmeyer N, Brandt S, Yamaoka Y, De Poire E, Sgouras D, Wessler S, Torres J, Smolka A, Backert S. c-Src and c-Abl kinases control hierarchic phosphorylation and function of the CagA effector protein in Western and East Asian Helicobacter pylori strains. J Clin Invest 2012;122:1553–1566.
17. Hase K, Murakami M, Iimura M, Cole SP, Horibe Y, Ohtake T, Obonyo M, Gallo RL, Eckmann L, Kagnoff MF. Expression of LL-37 by human gastric epithelial cells as a potential host defense mechanism against Helicobacter pylori. Gastroenterology 2003;125:1613–1625.
18. Yoshino N, Ishihara S, Rumi MA, Ortega-Cava CF, Yuki T, Kazumori H, Takazawa S, Okamoto H, Kadowaki Y, Kinoshita Y. Interleukin-8 regulates expression of Reg protein in Helicobacter pylori-infected gastric mucosa. Am J Gastroenterol 2005;100:2157–2166.
19. Akhiani AA, Pappo J, Kabok Z, Schon K, Gao W, Franzen LE, Lycke N. Protection against Helicobacter pylori infection following immunization is IL-12-dependent and mediated by Th1 cells. J Immunol 2002;169:6977–6984.
20. Sayi A, Kohler E, Hitzler I, Arnold I, Schwendener R, Rehrauer H, Muller A. The CD4+ T cell-mediated IFN-gamma response to Helicobacter infection is essential for clearance and determines gastric cancer risk. J Immunol 2009;182:7085–7101.
21. Le Martelot G, Claudel T, Gatfield D, Schaad O, Kornmann B, Lo Sasso G, Moschetta A, Schibler U. REV-ERBalpha participates in circadian SREBP signaling and bile acid homeostasis. PLoS Biol 2009;7:e1000181.
22. Woldt E, Sebti Y, Solt LA, Duhem C, Lancel S, Eeckhoute J, Hesselink MK, Paquet C, Delhaye S, Shin Y, Kamenecka TM, Schaart G, Lefebvre P, Nevière R, Burris TP, Schrauwen P, Staels B, Duez H. Rev-erb-alpha modulates skeletal muscle oxidative capacity by regulating mitochondrial biogenesis and autophagy. Nat Med 2013;19:1039–1046.
23. Li T, Eheim AL, Klein S, Uschner FE, Smith AC, Brandon-Warner E, Ghosh S, Bonkovsky HL, Trebicka J, Schrum LW. Novel role of nuclear receptor Rev-erbalpha in hepatic stellate cell activation: potential therapeutic target for liver injury. Hepatology 2014;59:2383–2396.
24. Yang G, Wright CJ, Hinson MD, Fernando AP, Sengupta S, Biswas C, La P, Dennery PA. Oxidative stress and inflammation modulate Rev-erbalpha signaling in the neonatal lung and affect circadian rhythmicity. Antioxid Redox Signal 2014;21:17–32.
25. Zhang L, Wu WK, Gallo RL, Fang EF, Hu W, Ling TK, Shen J, Chan RL, Lu L, Luo XM, Li MX, Chan KM, Yu J, Wong VW, Ng SC, Wong SH, Chan FK, Sung JJ,

Chan MT, Cho CH. Critical role of antimicrobial peptide cathelicidin for controlling Helicobacter pylori survival and infection. J Immunol 2016;196:1799–1809.
26. Sulli G, Rommel A, Wang X, Kolar MJ, Puca F, Saghatelian A, Plikus MV, Verma IM, Panda S. Pharmacological activation of REV-ERBs is lethal in cancer and oncogene-induced senescence. Nature 2018; 553:351–355.
27. Gibbs JE, Blaikley J, Beesley S, Matthews L, Simpson KD, Boyce SH, Farrow SN, Else KJ, Singh D, Ray DW, Loudon AS. The nuclear receptor REV-ERBalpha mediates circadian regulation of innate immunity through selective regulation of inflammatory cytokines. Proc Natl Acad Sci U S A 2012; 109:582–587.
28. Yu X, Rollins D, Ruhn KA, Stubblefield JJ, Green CB, Kashiwada M, Rothman PB, Takahashi JS, Hooper LV. TH17 cell differentiation is regulated by the circadian clock. Science 2013;342:727–730.
29. Sato S, Sakurai T, Ogasawara J, Takahashi M, Izawa T, Imaizumi K, Taniguchi N, Ohno H, Kizaki T. A circadian clock gene, Rev-erbalpha, modulates the inflammatory function of macrophages through the negative regulation of Ccl2 expression. J Immunol 2014;192:407–417.
30. Chen L, Li B, Yang WC, He JL, Li NY, Hu J, He YF, Yu S, Zhao Z, Luo P, Zhang JY, Li HB, Zeng M, Lu DS, Li BS, Guo H, Yang SM, Guo G, Mao XH, Chen W, Wu C, Zou QM. A dominant CD4(+) T-cell response to Helicobacter pylori reduces risk for gastric disease in humans. Gastroenterology 2013;144:591–600.
31. Molina-Infante J, Romano M, Fernandez-Bermejo M, Federico A, Gravina AG, Pozzati L, Garcia-Abadia E, Vinagre-Rodriguez G, Martinez-Alcala C, Hernandez-Alonso M, Miranda A, Iovene MR, Pazos-Pacheco C, Gisbert JP. Optimized nonbismuth quadruple therapies cure most patients with Helicobacter pylori infection in populations with high rates of antibiotic resistance. Gastroenterology 2013;145:121–128.e1.
32. Zhang W, Chen Q, Liang X, Liu W, Xiao S, Graham DY, Lu H. Bismuth, lansoprazole, amoxicillin and metronidazole or clarithromycin as first-line Helicobacter pylori therapy. Gut 2015;64:1715–1720.
33. Gerhart-Hines Z, Feng D, Emmett MJ, Everett LJ, Loro E, Briggs ER, Bugge A, Hou C, Ferrara C, Seale P, Pryma DA, Khurana TS, Lazar MA. The nuclear receptor Rev-erbalpha controls circadian thermogenic plasticity. Nature 2013;503:410–413.
34. Zhuang Y, Cheng P, Liu XF, Peng LS, Li BS, Wang TT, Chen N, Li WH, Shi Y, Chen W, Pang KC, Zeng M, Mao XH, Yang SM, Guo H, Guo G, Liu T, Zuo QF, Yang HJ, Yang LY, Mao FY, Lv YP, Zou QM. A pro-inflammatory role for Th22 cells in Helicobacter pylori-associated gastritis. Gut 2015; 64:1368–1378.
35. Lv YP, Cheng P, Zhang JY, Mao FY, Teng YS, Liu YG, Kong H, Wu XL, Hao CJ, Han B, Ma Q, Yang SM, Chen W, Peng LS, Wang TT, Zou QM, Zhuang Y. Helicobacter pylori-induced matrix metallopeptidase-10 promotes gastric bacterial colonization and gastritis. Sci Adv 2019;5:eaau6547.
36. Roussel Y, Wilks M, Harris A, Mein C, Tabaqchali S. Evaluation of DNA extraction methods from mouse stomachs for the quantification of H. pylori by real-time PCR. J Microbiol Methods 2005;62:71–81.
37. Mikula M, Dzwonek A, Jagusztyn-Krynicka K, Ostrowski J. Quantitative detection for low levels of Helicobacter pylori infection in experimentally infected mice by real-time PCR. J Microbiol Methods 2003; 55:351–359.

Received October 20, 2020. Accepted February 25, 2021.

Correspondence
Address correspondence to: Yuan Zhuang, National Engineering Research Center of Immunological Products, Department of Microbiology and Biochemical Pharmacy, College of Pharmacy and Laboratory Medicine, Third Military Medical University, No.30 Gaotanyan Street, Chongqing 400038, China. e-mail: yuanzhuang1983@yahoo.com; fax: (86)023-68752315.

CRediT Authorship Contributions
Fang-Yuan Mao (Investigation: Equal)
Yi-Pin Lv (Investigation: Supporting)
Chuan-Jie Hao (Investigation: Supporting)
Yong-Sheng Teng (Investigation: Supporting)
Yu-Gang Liu (Investigation: Supporting)
Ping Cheng (Investigation: Supporting)
Shi-Ming Yang (Resources: Supporting)
Weisan Chen (Writing – review & editing: Supporting)
Tao Liu (Investigation: Supporting)
Quan-Ming Zou (Investigation: Supporting)
Rui Xie (Investigation: Supporting)
Jing-Yu Xu (Investigation: Supporting)
Yuan Zhuang (Conceptualization: Lead; Funding acquisition: Lead; Investigation: Lead; Writing – original draft: Lead; Writing – review & editing: Lead)

Writing Assistance
None.

Conflicts of Interest
The authors disclose no conflicts.

Funding
This work was supported by the National Natural Science Foundation of China (Grant Nos. 81870394 and 82070578), the Chongqing National Science Fund for Distinguished Young Scholars (Grant No. cstc2019jcyjjqX0003), the National Key Research and Development Program of China (Grant No. 2016YFC1302200), and the Science Innovation Capacity Promotion Project of Army Medical University (Grant No. 2019XQY03).